Pathogenicity of Commensal Gut Biofilm In Prefrail Aging

Guillaume Le Cosquer[1,2], Melissa Pannier[1], Elodie Meunier[1], Julie Thevenin[1], Sophie Guyonnet[3,*], Bruno Vellas[3,*], Yohan Santin[4,*], Bruno Guiard[4,*], Angelo Parini[4,*], Louis Buscail[2], Barbara Bournet[2], Damien Guillemet[5], Celine Deraison[1], Nathalie Vergnolle[1,6,#,*], Jean-Paul Motta[1,#,*,✉] *for the IHU HealthAge INSPIRE/Open Science study group*

Affiliations:

[1]Institute of Digestive Health Research (IRSD), INSERM, Toulouse University, INRAe, ENVT, University Toulouse III Paul Sabatier (UPS), 31300 Toulouse, France

[2]Department of Gastroenterology and Pancreatology, Toulouse University Hospital (CHU Toulouse), Toulouse, France and Toulouse University, University Toulouse III Paul Sabatier (UPS), 31059 Toulouse, France

[3] Institute of Aging, Toulouse University Hospital (CHU Toulouse), Toulouse, France and CERPOP, Toulouse University, INSERM, University Toulouse III Paul Sabatier (UPS), 31300 Toulouse, France

[4] Institute of Metabolic and Cardiovascular Diseases (I2MC), INSERM, Toulouse University, University Toulouse III Paul Sabatier (UPS), 31432, Toulouse, France

[5] Nexira, 129 Chemin de Croisset, 76000 Rouen, France

[6] Department of Physiology and Pharmacology, University of Calgary Cumming School of Medicine, 3330 Hospital Drive, NW Calgary, AB, T2N4N1, Canada

* members of the IHU HealthAge INSPIRE/Open Science study group (full list in supplementary material)

[#] Co-supervision

✉Correspondence to: jean-paul.motta@inserm.fr

Keywords: gut microbiota; aging; microb-aging; gut biofilm; prefrailty; geroscience

Main text – ≈.6.700 words or ≈38.000 characters, excluding Title Page, Tables, Figures, and References

Abstract – 217 words

Display items – 6 Figures + 1 Table

Running title: Pathogenicity of prefrail gut biofilms

Abstract. Achieving healthy aging is a global challenge requiring a deeper understanding of aging mechanisms, spanning from robustness to frailty. Although age-related alteration of the gut microbiome (microb-aging) is well studied, there is a lack of research investigating the gut microbiota during the early stages of prefrailty and understanding its behavior within the context of a natural community lifestyle, in interaction with host tissue. Therefore, we used fecal samples from the human aging cohort INSPIRE-T, to characterize polymicrobial biofilms. Intestinal tissues and feces from an aging mouse cohort were also used. Food supplement was tested for potential geroprotective effects on biofilms. Findings pointed to taxonomic and physical alterations, increased instability, and virulence with regards to intestinal epithelium, for biofilms of prefrail individuals, compared to their age-matched robust counterparts. Multiparametric analyses further linked biofilm characteristics to clinical traits, suggesting that biofilm culture could be a proxy tool for evaluating a healthy or unhealthy aging status. Exposure of biofilms to the grape pomace prebiotic partially reversed the prefail biofilm phenotype. In aged mice with prefrailty, but not in robust aged mice, gut microbiota biofilm structure was altered and caused colon damage when transplanted into antibiotic-depleted mice. These findings suggest a causal link between microb-aging in prefrailty and gut inflammation, advocating microbiota-targeted therapies to reverse prefrail phenotype and thereby promote healthspan.

48 ## *1.* INTRODUCTION

49 By 2030, the World Health Organization (WHO) projects that one in six individuals
50 worldwide will be aged 60 years or older (World Health, 2020). This shift to older populations
51 coincides with an increase in age-associated diseases and unhealthy aging. One of the first
52 steps in the development of unhealthy aging is linked to the appearance of frailty syndrome,
53 a clinical condition defined as decreased physiological reserve and function that heightens
54 vulnerability and impairs the ability to withstand health stresses (Fried et al., 2001). The
55 absence of frailty (robust individuals) has been identified as a reliable predictor of prolonged
56 longevity without age-associated diseases (Romero-Ortuno & Kenny, 2012). The field of
57 geroscience, which has recently emerged, is dedicated to understanding the underlying
58 mechanisms of aging, finding methods to extend the healthspan – rather than lifespan – and
59 to delay or impede frailty syndrome and age-associated diseases (Sierra, 2016). The scientific
60 community has intensely focused on describing fecal microbiome composition and changes
61 in the aging population (Bosco & Noti, 2021; DeJong et al., 2020; Ghosh et al., 2022; O'Toole
62 & Jeffery, 2015). From these studies, it has become clear that chronological age is linked to
63 alterations within the gut microbiome, a process described as microb-aging (Bosco & Noti,
64 2021). A current challenge is to identify additional aspects of microb-aging, beyond
65 taxonomy, that could be related to early signs of unhealthy aging (in prefrail individuals)(Le
66 Cosquer et al., 2024). The involvement of microbiota behavior and virulence in such
67 differences has not yet been investigated. Although clinical scales allow geroclinicians to
68 categorize patients into three categories according to their frailty status (robust, prefrail, and
69 frail individuals), biological data on the relationship between these progressive clinical
70 changes and microb-aging dynamics are scarce. From a clinical perspective, prefrail
71 individuals represent a potentially reversible stage before a significant decline in health. A

72 report on community-dwelling elders indicated a notable prefrailty-to-robust transition, with
73 a 16% conversion rate observed over an 18-to 36-month follow-up period, compared to 0%
74 during the same period for the frailty-to-robust transition (Gill et al., 2006). Defining
75 conditions or treatments that would favor this transition from prefrailty-to-robust is among
76 the most important challenge of geroscience(Gill et al., 2006).

77 The motivation of this study was thus to focus on the aging population exhibiting prefrail
78 characteristics, in the search for interventions seeking at prefrailty-to-robust transition. For
79 that, we capitalized on the French INSPIRE-T cohorts at Toulouse University Hospital, two
80 clinically well-characterized human and mouse aging cohorts in which various non-invasive
81 samples were collected, including fecal samples. These cohorts were designed to identify
82 novel markers of aging, age-related diseases and health evolution that could be
83 therapeutically targetable (Ader et al., 2021; de Souto Barreto et al., 2021; Santin et al., 2021).
84 Considering its key importance on gut health and disease, we aimed at focusing on microbiota
85 communities living on the surface of the mucosa, as a polymicrobial anaerobic biofilm (Motta
86 et al., 2021). The underlying hypothesis was that microbial characteristics within biofilms
87 might undergo alterations not only with age but also with the health status of human donors.
88 Ultimately, our aim was to offer proof-of-concept geroprotective experimental approaches
89 to rectify these abnormalities.

90 2. MATERIALS & METHODS

91 *Human clinical data and samples*

92 This study used human feces collected from the INSPIRE-T cohort in 2021 (ID
93 NCT04224038) (de Souto Barreto et al., 2021). Donors were categorized into groups of 13
94 adults (7 men/6 women; 30-70 years) and 29 elderly subjects (+ 70 years). The last group was

95 divided into 14 prefrail (6 men/8 women) and 15 healthy or robust individuals (7 men/8
96 women). Frailty syndrome was evaluated using the Fried frailty index (see Supplementary
97 Table 2 for detailed Fried index calculation(Fried et al., 2001)). Donors were excluded if they
98 had received antibiotics, probiotics, or prebiotics within the past three months and if they
99 had history of any of the following conditions: inflammatory bowel disease, irritable bowel
100 syndrome, colorectal cancer, immunosuppression, severe liver disease. Feces were collected
101 at the initial visit, aliquoted (≈1 g), and stored at −80°C until analysis in the INSPIRE-T biobank
102 at a central laboratory (Toulouse Bio Ressources CRB , CHU Toulouse/IFB Purpan, Toulouse,
103 France). Clinical characteristics, including age, gender, frailty status, and household status,
104 were documented (Supplementary Table 1: lifestyle). For the present analysis, we used the
105 version 1.0 of the INSPIRE-T database. We calculated the nutritional status of each individual
106 using the Mini Nutritional Assessment (MNA; Supplementary Tables 3 and 4(Rubenstein et
107 al., 2001)) and calculated the Charlson Comorbidity Index based on their past medical
108 history(Charlson et al., 1987)(Supplementary Tables 5, 6, and 7). Full list of members of the
109 IHU HealthAge INSPIRE/Open Science study group is included in Supplementary Material.

110 *Mouse functional data and samples*

111 This study involved colon tissue and feces collected from the INSPIRE mouse cohort
112 (CREFRE – US006 / Inserm – University of Toulouse, Paul Sabatier). The cohort comprised male
113 and female SWISS outbred mice(Santin et al., 2021). Animals underwent health assessments
114 to measure frailty, using a rodent equivalent to the human Fried frailty index, the Valencia
115 Score(Gomez-Cabrera et al., 2017; Santin et al., 2021) (Supplementary Table 8). Behavioral
116 phenotyping was conducted by the Mouse Behavioral Core platform (Integrative Biology
117 Center, CBI, Toulouse), at the CREFRE facility. In this study, we collected samples from young
118 (6 months, n=8), aged robust (24 months, n=8), and aged prefrail animals (24 months, n=8).

119 Distal colon was fixed in methacarn solution (6/3/1 of methanol/chloroform/acetic acid), and
120 embedded in paraffin. Feces were collected and stored at −80°C. Both paraffin blocks and
121 frozen feces were maintained in the INSPIRE mouse biobank at a central laboratory (Centre
122 de Ressources Biologiques-Cancer - Institut Universitaire du Cancer Toulouse – Oncopole,
123 CHU Toulouse, Toulouse, France).

124 *Culture of biofilms from human feces*

125 Human fecal samples (10-20 mg) were resuspended in supplemented Brain Heart Infusion
126 (BHI, Sigma-Aldrich, St. Quentin Fallavier, France) as described in(Motta et al., 2018; Motta et
127 al., 2019; Motta et al., 2015). Biofilms were generated using an MBEC Assay® (Innovotech,
128 Edmonton, Canada) with identical initial densities for each donors (OD600nm= 0.1). MBEC
129 plates were pre-coated overnight at room temperature with gastric porcine mucin (10 mg/ml,
130 Sigma-Aldrich). After 72 h of maturation, the biofilm biomass, viability, and matrix content
131 were characterized as described below. Alternatively, the medium was refreshed for 24h to
132 collect biofilm-dispersed bacteria for 16S rDNA metabarcoding, to estimate the rate of
133 dispersal, and to perform interaction assays with human intestinal epithelial cells. Short-term
134 microbiological handling was performed in a hypoxic chamber (0.1% oxygen; Don Whitley
135 H35; Bingley, UK). Longer incubations were performed at 37°C in an anaerobic chamber (Don
136 Whitley A20) or hermetic jars with an anaerobic sachet (Anaeropack, Thermo Fisher).

137 *Staining assays on MBEC biofilm plates*

138 Total biofilm biomass was evaluated using Gram's safranin-O solution (Sigma-Aldrich),
139 biofilm matrix-associated sugar content using fluorescein wheat germ agglutinin (WGA, 1/100
140 diluted, ThermoFisher), and viability using a resazurin assay (1 mg/ml; Sigma-Aldrich)(Motta
141 et al., 2018; Motta et al., 2019; Motta et al., 2015). The dispersal rate was estimated at 24h
142 by measuring the ratio of viable biofilm-dispersed bacteria to total biofilm biomass. Briefly,

143 MBEC were transferred to 96 well plate containing stains and incubated at 37°C for 2 h
144 (resazurin and WGA) or 20' (safranin-O). Stains were recovered by sonication at 45 kHz (USC-
145 500T, VWR) in a plate containing acetic acid (30%, safranin-O) or 1.5M sodium chloride
146 (WGA). Specific absorbance (safranin-O) or fluorescence (WGA and resazurin) was measured
147 using an EnSight spectrophotometer (Perkin Elmer, Villepinte, France). An average of at least
148 12 biofilm replicates were performed for each individual. A positive control was included for
149 each experiment (*E. Coli* LF82, a high biofilm producer).

150 *In vivo transplantation: Donor microbiota preparation*

151 Feces obtained from SWISS aged mice were divided into three groups of interest: young
152 (n=8 mice, 4 males and 4 females, 6 months old), aged robust (n=8 mice, 5 males and 3
153 females, 24 months old), and aged prefrail (n=8 mice, 5 males and 3 females, 24 months
154 old(Santin et al., 2021)). Feces were pooled in 1.5 mL phosphate buffered saline (PBS, Eurobio
155 Scientific, Les Ulis, France), homogenized, and filtered through a sterile nylon mesh strainer.
156 The filtered contents were centrifuged twice, and the pellet was resuspended in PBS/20%
157 glycerol at OD_{600nm}=1.5 (≈10^9 CFU/ml). All the procedures were performed under anaerobic
158 conditions at 37°C in an anaerobic chamber (Don Whitley A20).

159 *In vivo transplantation: Post-antibiotics fecal microbiota transfer (FMT)*

160 C57BL/6 mice (Janvier, Le Genest Saint-Isle, France), aged 8 weeks, were housed under
161 specific pathogen-free conditions (CREFRE U006, CHU Purpan). Mice were assigned to three
162 experimental cages: FMT-6M (n=9), FMT-24M robust (n=8), and FMT-24M prefrail (n=7), and
163 acclimatized for 2 weeks before the experiment. The existing microbiota was depleted by
164 broad-spectrum antibiotics in drinking water at concentrations of 1 g/l (ampicillin and
165 metronidazole, Sigma-Aldrich) and 0.5 g/l (neomycin and vancomycin, Sigma-Aldrich) for the
166 first five days, and half-diluted for the remaining days. On day 10, the mice underwent FMT

167 via oral gavage with 200 µL of previously described fecal slurry. Four days post-
168 transplantation, the colon was harvested for evaluation of macroscopic damage, including
169 colon thickness edema (in mm) and blind Wallace scoring endpoints(Wallace et al., 1995),
170 was assessed by a blinded and skilled experimenter. Animal procedures were approved by
171 the National Laboratory Animal Ethics Committee (APAFIS 2023060610225611, French
172 Ministry of Research).

173 *16S rDNA amplicon sequencing*

174 Total DNA was extracted from feces or biofilms using the EZNA isolation kit stool DNA
175 (VWR for biofilms) according to the manufacturer's protocol. DNA extraction and specific PCR
176 amplification of 16S bacterial rDNA V3-V4 regions were targeted by 341f-806R primers and
177 sequenced on the Illumina MiSeq 2 × 250 bp technology at Vaiomer (Toulouse, France) or
178 Biomnigene (Besancon, France). Demultiplexed raw read sequences were processed using
179 FROGS bioinformatics pipeline (FROGS v. 4.1.0(Bernard et al., 2021), Galaxy Toulouse server,
180 GenoToul). Adaptor and primer sequences were trimmed, and amplicons were merged using
181 Vsearch plugin (v.2.17.0). Cluster filtering and denoising (swarm v2.0) plugins were then used
182 for quality control and identification of amplicon sequence variants (ASVs). Taxonomic
183 assignments were performed using the 16S SILVA 138.1 database.

184 *16S rDNA Fluorescent In situ hybridization (FISH)*

185 For fluorescence in situ hybridization (FISH), methacarn-fixed mouse colon tissues were
186 embedded in paraffin. Slides were hybridized with a universal bacterial 16S fluorescent rRNA
187 probe (EUB338-Cy3, 5'GCTGCCTCCCGTAGGAGT-Cy5, Eurofins Scientific, France) and DNA was
188 counterstained with 4',6-diamidino-2-phenylindole (DAPI, Invitrogen) and polysaccharide
189 content (wheat germ agglutinin labeled with fluorescein, ThermoFisher)(Motta et al., 2018;
190 Motta et al., 2019). The biofilm damage score was blindly evaluated in at least three

191 microscopic fields for each mouse in the groups of interest, according to the criteria described
192 in(Motta et al., 2019). Samples that were unsatisfactorily fixed for scoring were excluded from
193 analysis. Images were acquired using a Leica LSM 710 confocal microscope (TRI Genotoul,
194 Purpan), and FIJI freeware was used for the final image mounting (v.1.51, Mac Os).

195 *Human intestinal epithelial cells*

196 Caco-2 (ATCC, Manassas, USA) and HT29-MTX E12 (ATCC) were grown separately in
197 Dulbecco's modified Eagle medium (DMEM, Eurobio Scientific, Les Ulis, France)
198 supplemented with 10% fetal bovine serum (FBS, Sigma-Aldrich), penicillin/streptomycin
199 (Invitrogen, Massy, France) and non-essential amino acid solution (Thermofisher, Paisley, UK)
200 at 37°C in a humidified incubator with 5% CO2 as previously described (Rolland-Fourcade et
201 al., 2017). Coculture at 3:1 (Caco-2:HT29) was done on flat bottom 24-wells plates at an initial
202 total density of 2.10^5 cell per well (Corning, Thermo Scientific). Cells were screened for
203 mycoplasma infection (MycoAlertTM, Lonza, Bâle, Switzerland) and treated before coculture
204 if necessary (PlasmocureTM, Lonza). Cells were cocultured with dispersed bacteria from
205 biofilms (normalized optical density; OD_{600nm}=0.01) in OPTIMEM (Thermo Fisher). Bacterial
206 adhesion to the intestinal epithelium was assessed after 4 h of coculture on a blood agar
207 plate(Motta et al., 2018; Motta et al., 2019).

208 *Relative mRNA expression by qRT-PCR*

209 Total RNA was extracted using TRIzol reagent (Euromedex, France) after 4 h of coculture
210 (Qiagen, Montreal, Canada). Reverse transcription of isolated RNA was performed using the
211 Maxima First Strand Kit (Invitrogen, Thermo Scientific) according to the manufacturer's
212 instructions. Quantitative PCR (RT^2qPCR Primer, Qiagen) was performed on a LightCycler
213 (Roche, Basel, Switzerland) based on SYBR Green technology, using the Takyon Low Rox SYBR
214 kit (Eurogentec, Seraing, Belgium). Data were analyzed by the $2^{-\Delta\Delta CT}$ method using HPRT and

215 GAPDH (Qiagen) as control genes and expressed as fold change compared to control cells
216 without bacteria. PCR primers used in this study are listed in Supplementary Table 9.

217 *Grape pomace (prebiotic) intervention*

218 After maturation, MBEC Assay® was exposed to grape pomace solution diluted in
219 microbiological BHI supplemented broth at several concentrations (0.3 to 30 mg/mL) for 24h.
220 The medium was refreshed, and 4h later dispersed bacteria were collected to collect biofilm-
221 dispersed bacteria for interaction assays with human intestinal epithelial cells. Staining assays
222 were performed in parallel to estimate the effect of grape pomace on biofilm biomass and
223 matrix-associated sugar content. The industrial grape pomace used (VinOgrape™, Nexira,
224 France) was an extract containing purified polyphenols (>90% content, quantified by
225 spectrophotometry method) anthocyanins, catechin, epicatechin and oligomeric
226 proanthocyanidins.

227 *Statistics and visualization*

228 We performed statistical analyses and data visualization using R 4.3.0 – Posit (Rstudio IDE)
229 v2023.0.9.1 built 494 (Posit Team 2023, Boston, MA, USA) and GraphPad Prism (v10 for
230 MacOs, La Jolla, USA). Baseline clinical characteristics were compared between the groups
231 with chi-squared test for categorical variables and ANOVA (Fisher test) for continuous
232 variables with Tukey's method to correct P-values.

233 To explore the bacterial taxonomy variability among sample groups, alpha and beta
234 diversity metrics were performed in R using phyloseq (v.1.46.0). Principal coordinate analysis
235 (PCoA) and principal component analysis (PCA) were performed in R using phyloseq (v. 1.46.0)
236 and compared using PERMANOVA (pairwiseAdonis v.0.4.1) with 9999 permutations. Taxa bar
237 plots were generated in R using phyloseq (v. 1.46.0) and ggnested (v. 0.1.0). Statistical
238 differences between microbial communities were assessed in R using LEfSe (lefser

239 v.1.12(Segata et al., 2011)), Deseq2 (v.1.42(Love et al., 2014)), EdgeR (v.4.0.3(Robinson et al.,
240 2010)), metagenomeSeq (v.1.43.0(Paulson et al., 2013), and ANCOM(Mandal et al., 2015).
241 Boxplots, barplots and scatter plots were generated in R using ggplot2 (v.3.4.4) and ggpubr
242 (v.0.6.0).

243 Heatmaps were created in R using complexheatmap (v.2.18.0). Grout's test was used to
244 filter statistical outliers in the qPCR dataset (GraphPad Prism). Statistical significance was set
245 at $P < 0.05$. For group comparisons, we used Dunnett's or Tukey's method to correct P-values
246 for ANOVA and the Benjamini-Hochberg method for differential abundant taxa analyses.
247 Unless otherwise indicated, values are presented as the mean ± standard error of the mean.

248 3. RESULTS

249 Characterization of the human cohort

250 Samples were collected from 42 individuals, stratified into 13 healthy individuals aged 30-
251 70 years and 29 individuals aged ≥ 70 years. Within the aged group, 15 were robust based on
252 the Fried frailty index(Fried et al., 2001), while 14 were prefrail (score of 1 and 2) (Table 1 and
253 Supplementary Table 1). All the donors had satisfactory nutritional scores (Supplementary
254 Table 3). As expected, the Charlson comorbidity index (Charlson et al., 1987) indicated more
255 comorbidities in aged individuals than in younger donors (0.923±1.19 versus 4.73±1.87,
256 $P<0.001$), but this index was not discriminant between prefrail and robust donors (5.07±1.59
257 versus 4.73±1.87, $p=0.836$; Supplementary Table 6). General characteristics of donors used in
258 the study are summarized in Table 1.

259 Taxonomic characterization of microb-aging on human biofilms

260 To explore links between microb-aging and prefrailty syndrome, we cultured the fecal
261 microbiota of aged individuals on a mucin-coated device, in an attempt to reproduce a

262 mucosal polymicrobial anaerobic biofilm (Motta et al., 2021). Using 16S V3-V4
263 metabarcoding, we identified that microbial community was dominated by Bacillota
264 (formerly Firmicutes), followed by Actinobacteria and Bacteroidota (formerly Bacteroidetes).
265 At Family level, biofilm core taxa belong to *Ruminococcaceae*, *Christensenellaceae,*
266 *Bifidobacteriaceae, Akkermansiaceae, Lachnospiraceae*, and *Oscillospiraceae* (Fig.1A,
267 Supplementary Fig.1). Being a recognized hallmark of human microb-aging, we confirmed
268 that biofilms from aged donors had reduced α-diversity compared to 30-70 years old
269 individuals (Chao1, ACE, Simpson, Shannon, and Fisher indices, Fig.1B). Following with β-
270 diversity analyses (Fig. 1C, Supplementary Fig. 1B), we found that biofilms from aged robust
271 donors exhibited heightened individual microbiome uniqueness compared with those from
272 prefrail. Regarding the relative abundance distribution at the Family level, no hierarchical
273 clustering was evident among the donor groups or with the Fried frailty index (Supplementary
274 Fig.1A). We then ran various statistical models in 16S metagenomics to identify differentially
275 abundant taxa (i.e., Deseq2, metagenomeSeq, ANCOM, and edgeR, Supplementary Tables 10
276 and 11, Supplementary Fig.1). Importantly, we found correspondence in age-related taxa
277 abundance between the biofilm model and other reports on human aging cohorts(Bosco &
278 Noti, 2021; DeJong et al., 2020; Ghosh et al., 2022; O'Toole & Jeffery, 2015) (Supplementary
279 Fig.1C, 1D). Specifically, aged individuals presented an enrichment of taxa including
280 *Selemonadaceae*, *Prevotellaceae*, and potential pathobionts such as *Enterobacteriaceae*.
281 Concomitantly, there was a reduction in the abundance of important commensals within aged
282 biofilms, including *Dialister sp., Akkermansia sp.* and *Bifidobacteriaceae* (Supplementary
283 Fig.1C). Biofilms from aged robust individuals displayed a higher abundance of *Prevotellaceae*
284 compared to prefrail individuals, as well as an increased representation of *Selenomonadaceae*
285 *(Megamonas sp.)* and *Ruminococcaceae* (Supplementary Fig.1D).

286 We then expanded the investigation between clinical characteristics of donors and taxa
287 abundance in the biofilm model. Employing Kendall's correlation approach and excluding
288 non-statistically significant scores, we identified 34 taxonomic biofilm features, primarily at
289 the Family and Genus levels, that were significantly associated with clinical characteristics
290 (Fig.1D). First, aging alone was linked to a diminished abundance of core taxa such as *Slackia*
291 *sp.*, *Eggerthellaceae*, and Bifidobacteriales. In addition, we found a positive correlation
292 between prefrailty and the relative abundance of *Monogobales, Oscillibacter sp.* and
293 *Negativibacillus sp.* Regarding clinical history, the Charlson comorbidity index was negatively
294 correlated with abundance of *Slackia sp*., and *Veillonellaceae (Dialister sp.)*. Abundances of
295 *Pasteurellaceae* and *Haemophilus sp.* were inversely correlated with the MNA score, shedding
296 light on the potential links between these specific taxa and nutritional status. Gender
297 exhibited no statistically significant correlation with the abundance of microbial taxa in
298 cultured biofilms. Finally, regarding the living conditions of donors, we uncovered a positive
299 correlation between conjugal lifestyle and the microbial abundance of several taxa, including
300 *Tannerellaceae*, *Parabacteroides sp.*, and *Butyricimonas sp.* In summary, these findings
301 indicate that biofilms derived from fecal samples harbor alterations indicative of microb-
302 aging, with a reduced abundance of core taxa members coupled with an increased abundance
303 of Proteobacteria. Importantly, *cultured* biofilm maintains specific composition related to the
304 prefrailty status of their donors. In addition to these taxonomic observations, this culture
305 approach allowed us to further elucidate the structural and behavioral features of microb-
306 aging.

307 **Physical structure of human biofilms is altered in prefrail donors**

308 To explore microb-aging beyond taxonomy, we first characterized the physical structure
309 of biofilms. We observed a negative correlation between donor age and total biofilm biomass

310 (Pearson R = -0.6, P<0.05, Fig.2A). However, this feature was not significantly different
311 between prefrail and robust biofilms (Fig.2B). Regarding the extracellular matrix of biofilms,
312 we found a positive correlation (R=0.39, P<0.05) between age and proportion of sugar within
313 this matrix (Fig.2D). Interestingly, biofilms from prefrail donors exhibited a heightened sugar
314 matrix composition compared to the other samples (Fig.2E). We then investigated the links
315 between the clinical characteristics of human donors and biofilm physical structure (Kendall's
316 correlation approach, Fig.2C). In addition to confirming the previously described Fried and
317 age relationship, we found a negative correlation between biofilm biomass and the Charlson
318 comorbidity index (Fig.2C). Neither the donor's sex, household, nor diet (MNAscore)
319 demonstrated a significant association with the biofilm structure (Fig.2C). Focusing on biofilm
320 taxonomy (Fig.2F), we identified that high biomass biofilm, a feature of 30-70 yrs biofilms,
321 was positively correlated with a high abundance of *Eggerthellaceae*, *Oscillospira sp.*,
322 *Enterorhabdus sp.*, and *Slackia sp.* High biofilm matrix-sugar, a feature of prefrail biofilms,
323 was correlated with donors harboring low abundance of Coriobacteriales and
324 *Eggerthellaceae* (Fig.2F). Overall, these observations suggest that the physical structure of
325 biofilms generated from 30-70 and aged individuals differs and, more importantly, that these
326 physical modifications may serve as discriminant features between aged individuals
327 predisposed to prefrailty or robustness.

328 **Prefrailty-associated human biofilms have an hypervirulent phenotype**

329 In addition to the physical structure, we evaluated the pathogenic behavior of human
330 biofilms between young and aged donors. First, we assessed the stability of biofilms,
331 measured as the rate of bacterial dispersal over a 24-hour period. High dispersal is considered
332 a virulent trait that increases the likelihood of exposing the subjacent host epithelium to
333 unwanted bacterial contact (Motta et al., 2018; Motta et al., 2015). Donor age was not

334 statistically correlated with this feature (P=0.058, Fig.3A). However, prefrail biofilms had a
335 significantly higher dispersal rate than biofilms from younger groups (P<0.05, Fig.3B). We then
336 explored the ability of biofilms to disperse bacteria that could attach to the underlying
337 intestinal epithelium. To this end, we exposed enterocyte/mucus-producing human epithelial
338 cell lines to a normalized concentration of the dispersed biofilm bacteria. We found that
339 higher chronological age correlated with this behavior (P<0.05, Fig.3D). More importantly, it
340 was dispersed bacteria from prefrail biofilms that exhibited heightened adhesiveness
341 compared to other groups (P<0.01, Fig.3E). Intriguingly, the adhesiveness of bacteria was
342 correlated with individuals having a high Charlson comorbidity index, suggesting a potential
343 connection between bacterial behavior and clinical history (Fig.3C). In this cohort, neither the
344 donor's gender, household, nor diet (MNA score) demonstrated a statistically significant
345 correlation's index with biofilm pathogenic behavior (Fig.3C). Regarding taxonomy, biofilm
346 dispersal was statistically correlated with a lower abundance of *Ruminococcaceae* and
347 *Oscillospirales sp*. In addition, we identified several taxa whose abundance was either
348 positively (e.g., *Adlercreutzia sp.* and Coriobacteriales) or negatively (e.g., *Akkermansiaceae*)
349 correlated with biofilm bacterial adhesiveness (Fig.3F). In summary, our findings underscore
350 that while chronological age plays a limited role in influencing biofilm behaviors, prefrailty
351 status emerges as a key factor shaping the instability and virulence of gut biofilms.

352 **Prefrailty-associated biofilms trigger host innate response in human intestinal**
353 **epithelium**

354 We then focused on the relative expression of 10 genes encoding proinflammatory
355 cytokines, antimicrobials, and tight junction proteins to discern patterns indicative of the host
356 epithelial innate response to these biofilm-dispersed bacteria. The scaled expression
357 heatmap revealed not only altered expression patterns in biofilms from aged versus younger

358 individuals, but also striking disparities within biofilms from prefrail versus robust individuals
359 (Fig.4A). Proinflammatory genes, such as *IL6* and *TNF*, and the tight junction genes claudin-2
360 (*CLDN2*) and occludin (*OCLN*) (Fig.4B) exhibited a notable trend towards increased expression
361 in prefrail versus robust individuals. While such trends failed to reach statistical significance
362 when considered alone – except in the case of *TNF* and *IL6* – the PCA ordination plot
363 demonstrated a clear shift in the transcriptome of epithelia exposed to bacteria from prefrail
364 individuals compared to younger individuals (Fig.4C, PERMANOVA P= 0.007). As visualized in
365 the biplot vectors, genes with the greatest contribution in the separation were those coding
366 for proinflammatory signals (*TNF*, *IL8 and IL6* along the PC1 axis) and those related to tight
367 junction proteins (*CLDN2* and *OCLN* in the PC2 axis). Expanding this analysis with biofilm
368 features, we discovered that high dispersal rate – indicative of a virulent prefrail phenotype
369 – was correlated with a higher expression of inflammatory genes (*IL6* and *TNF*, Fig.4D).
370 Interestingly, high adhesiveness was also positively correlated with inflammatory genes
371 (*COX2*) as well as genes encoding tight junction proteins (*CLDN2* and *OCLDN*; Fig.4C). Finally,
372 we found that an increased quantity of sugar in the biofilm matrix – a feature linked to aging
373 and prefrailty – was positively correlated with a higher expression of proinflammatory genes
374 (*IL6*, *IL8*, and *TNF*). Overall, these findings indicate that in addition to aging host immunity,
375 microbiota biofilms from +70 years prefrail individuals, but not in 30-70 years and +70 years
376 robust individuals, contain commensals with proinflammatory triggering potential.

377 **Prefrailty aging in mice is linked to altered mucosal biofilm biogeography in colon.**

378 Motivated by *cultured* human biofilm models, we aimed to confirm whether early signs of
379 prefrailty could influence the spatial organization of the gut microbiota in the colon. For this,
380 we used tissues from an aging mouse cohort, equivalent to humans aged 30 to 70+ years (= 6
381 to 24 months old, INSPIRE mouse cohort(Santin et al., 2021)). Among the 15 selected animals,

382 thorough frailty syndrome assessments were conducted, categorizing them into groups
383 mirroring healthy aging (robust, n=8) and those displaying early signs of frailty (prefrail, n=7,
384 Valencia Frailty Score, Supplementary Table 8(Gomez-Cabrera et al., 2017)). Upon sacrifice,
385 the colon-associated microbiota was visualized using 16S rDNA fluorescent *in situ*
386 hybridization (FISH) staining (Fig.5A). Remarkably, young mice exhibited a mucosal microbiota
387 organized as a dense biofilm community lining a layer of sterile mucus (outlined by dashed
388 lines in yellow, Fig.5A). In contrast, aged animals displayed a different spatial organization,
389 featuring isolated bacteria within the mucus layer that escaped from the dense mucosal
390 biofilm (arrows, Fig.5B and 5C). Bacterial translocation, which was almost absent in the young
391 cohort, was observed in the aged animals (Fig.5B and 5C). Notably, aged prefrail animals
392 exhibited more signs of tissue-associated biofilm alterations than aged robust animals,
393 including signs of virulent behavior in gut microbiota such as invasion of the mucus sterile
394 layer, epithelial adhesion, or translocation (biofilm damage score(Motta et al., 2019), Fig.5D).
395 These findings confirmed *in vivo* that prefrail status in aging is linked to altered biofilm
396 organization and emergence of virulent phenotypes.

397 **Prefrailty-associated microbiota directly causes colon damage when transplanted into**
398 **young mice**

399 To experimentally demonstrate a causal relationship between prefrailty-associated
400 microbiota and local gut inflammation, we conducted fecal microbiota transplantation (FMT)
401 in antibiotic-treated young mice. We used as transplant a pool of feces from young (6 months,
402 n=8), robust (24 months, n=8), and prefrail mice (24 months, n=8). As expected, the antibiotic
403 regimen caused transient dysbiosis in microbiota, with an increased abundance of
404 *Enterobacteriaceae*, which was partially restored after 4 days of antibiotic washout (Fig.5E
405 and Supplementary Fig.2). In recipient mice, the fecal 16S composition of FMT-prefrail was

406 significantly different from that of mice that underwent FMT with young and aged robust
407 microbiota (Fig.5E, Supplementary Fig.3 and 4). Mirroring previous findings in aging mice
408 (Langille et al., 2014) – as well as our own findings in human biofilms – mice transplanted with
409 prefrail microbiota conserved a significantly higher abundance of harmful Proteobacteria
410 taxa, combined with a reduced abundance of core commensal taxa (*Muribaculaceae*,
411 *Christensenellaceae*, *Parabactoides sp.* and *Akkermansia sp.*, Supplementary Fig.4). Regarding
412 intestinal tissue damage after the FMT procedure, we found that young fecal microbiota did
413 not cause macroscopic harm in the colon (total damage score of 1.7±0.44, Fig.5F-G). However,
414 when exposed to aged microbiota FMT, recipient animals had significantly higher colon
415 damage such as increased incidence of erythema, mucus release in the lumen, edema, and
416 ulcers (1.7±0.44 vs. 3.6±0.73, P= 0.035, Fig.5F-G). Further stratifying aged animals into robust
417 and prefrail categories revealed a substantially higher damage score in the prefrail group
418 compared to robust animals (total score 5.4±0.98 vs. 2±0.98, ANOVA followed by Dunnett's
419 test, P = 0.002, Fig.5G). These results combined with previous *in vitro* assays, confirmed that
420 microbiota from prefrail – but not from young and robust – directly causes intestinal damage
421 when transplanted into recipient young mice.

422 **Grape pomace partially reverses prefrailty-associated biofilm structure and virulence**

423 Considering the virulent phenotype of the prefrail microbiota and its associated damage
424 to the intestinal mucosa, we investigated whether this phenotype can be reversed by
425 microbiota-targeted strategies. Grape-derived polyphenols have long demonstrated
426 prebiotic properties via their activities on gut microbes (Davinelli & Scapagnini, 2022; Luo et
427 al., 2021; Xu et al., 2021; Ziegler et al., 2023). Indeed, the majority of edible grape polyphenols
428 are poorly bioavailable and reach the colonic compartment where they shape microbiome
429 profile (Rodriguez-Lopez et al., 2022). Therefore, we sought to determine whether industrial

430 grape pomace, which is already marketed as a food supplement in France, can affect the
431 structure and virulence of mucosal biofilms associated with prefrail aging. Focusing on the
432 discriminant biofilm features described above in the aged human biofilms, we found that the
433 grape pomace extracts restored the biomass of prefrail biofilms, at a level similar to that
434 found in biofilms from healthy individuals (Fig.6A, $P<0.001$ at 30 mg/ml). Importantly, we
435 found a statistically significant reduction of 79.5% in the dispersal rate in prefrail biofilms,
436 returning to the level recorded in biofilms from robust individuals (Fig.6B, $P<0.05$ at 30
437 mg/ml). Grape pomace had no significant effect on the increased adhesiveness of dispersed
438 bacteria from prefrail biofilms (Fig.6C). At a concentration of 30 mg/ml, biofilm exposure to
439 grape pomace led to a significant reduction of dispersed bacteria able to trigger the
440 expression of *TNF* (55% reduction, $P<0.05$, Fig.6D) or *IL6* (43.9% reduction, $P>0.05$, Fig.6E),
441 while having no impact on *IL8* ($P>0.05$, Fig.6F). Overall, these experiments using a biofilm
442 model suggested that grape pomace could directly reduce the hypervirulent phenotype
443 associated with the prefrail aging microbiota.

444 **4. DISCUSSION**

445 Aging is commonly associated with changes in the gut microbiota, including shifts in
446 taxonomy and metabolism, a phenomenon referred to as microb-aging (Bosco & Noti, 2021).
447 Despite extensive research on fecal microbiome from various populations worldwide
448 (reviewed in(Bosco & Noti, 2021; DeJong et al., 2020; Ghosh et al., 2022; O'Toole & Jeffery,
449 2015)), significant knowledge gaps remain on the ecological implications of microb-aging
450 within commensal gut communities. Another under-explored area is the causal relationship
451 between microb-aging and low-grade inflammation of aging (Franceschi et al., 2018; Le
452 Cosquer et al., 2024). Additionally, the role of microbiota in frailty aging and the potential of

453 microbiota-targeted therapies in transitioning from prefrailty to robustness remain open
454 questions. Addressing these gaps is crucial for understanding the nature of microb-aging and
455 identifying non-chronological markers of unhealthy aging (Ader et al., 2021; Sierra, 2016).
456 Using non-invasive samples in a clinically well characterized human aging cohort, we thus
457 aimed at generating a model for microbiota forming biofilm, which is the microbial lifestyle
458 that resides in close proximity to the host tissue and epithelium (Motta et al., 2021). In this
459 study, we aimed at detecting microbiome shifts in biofilms from aged individuals at an early
460 stage of frailty, specifically to uncover potential therapeutic interventions that can reverse
461 these changes and establish new targets that promote the transition from prefrailty to
462 robustness (Gill et al., 2006).

463 From a taxonomic and alpha-diversity perspective, the cultured biofilm maintained
464 important microb-aging features already described in the literature, such as reduced alpha-
465 diversity (Fig.1B)(Bosco & Noti, 2021; Ghosh et al., 2022; Jackson et al., 2016; Maffei et al.,
466 2017; O'Toole & Jeffery, 2015), as well as increased microbiome uniqueness in robust but not
467 in prefrail aged individuals (Fig.1D)(Wilmanski et al., 2021). By comparing biofilm taxonomy
468 results with a recent grouping proposed by Ghosh et al.(Ghosh et al., 2022) — Groups I, II,
469 and III—we observed an interesting parallelism, where gut pathobionts, such as
470 Proteobacteria from the *Enterobacteriaceae* family, exhibited increased abundance in aged
471 individuals. We also noted a decline of beneficial taxa in aged biofilms, such as
472 *Bifidobacteriaceae*. Interestingly, *Akkermansia sp.*, a genus containing important commensals
473 involved in host/mucus homeostasis(Cani et al., 2022), showed slightly reduced abundance
474 in aged biofilms. Intriguingly, biofilms from aged robust individuals displayed increased taxa
475 traditionally associated with cohorts of healthy centenarians such as *Christencellaneaceae*
476 (Biagi et al., 2016; Biagi et al., 2010; Kong et al., 2016). Other disparities between robust and

477 prefrail individuals were also observed (Fig.2B), with taxa producing short-chain fatty acids
478 (SCFAs) being more abundant in biofilms from robust individuals (e.g., *Prevotellaceae*).
479 Interestingly, biofilms from prefrail donors displayed a slightly higher abundance of disease-
480 associated taxa such as *Megamonas* species, compared to robust donors biofilm (Fig.2B). As
481 a limitation of these taxonomy findings relates to small sample size, further investigation
482 within the entire INSPIRE cohort could be engaged to confirm and refine the identified
483 taxonomic features (+1000 volunteers, (de Souto Barreto et al., 2021)). In addition, the
484 longitudinal design of this cohort will enable collection from the same individuals over the
485 next 10 years, enabling us to track the progression of prefrailty in individuals and determine
486 whether they experience a shift to frailty, provided that microb-aging is not therapeutically
487 managed (with diet, exercise or pre- and probiotics).

488 In addition to taxonomic alterations, this study revealed new microbiological features that
489 may help distinguish between healthy and unhealthy aging in humans. Specifically, we
490 identified a reduced biofilm-forming capacity in most fecal samples of aged individuals
491 compared to that in younger individuals (Fig.3). This may indicate a common biological
492 pattern in the aging microbiome that is potentially linked to the loss or gain of specific taxa,
493 as previously discussed. More compelling are those features that distinguish between aged-
494 matched robust and prefrail donors, such as the amount of sugar associated with the biofilm
495 matrix (Fig.3). Extracellular polysaccharides are fundamental for retaining water within the
496 biofilm matrix, generating a highly hydrated and cohesive environment that influences cell
497 movement (Flemming & Wingender, 2010; Karygianni et al., 2020). Whether the altered sugar
498 composition of the aged prefrail biofilms used in the present study contributes to taxonomic
499 changes, increased dispersal, and fragmented biofilm physical structure *in vitro* (Fig.3) and *in*
500 *vivo* (Fig.6) remains to be experimentally elucidated. Another discriminant feature of

501 prefrailty-associated biofilms is their capacity to release bacteria with higher adhesiveness
502 and which triggers proinflammatory signals from the underlying epithelium (Fig.4). Although
503 this phenomenon has not been previously documented, metagenomic studies of fecal
504 microbiota have indicated an increased proportion of virulence gene pathways in microbiota
505 from aged frail individuals (Maffei et al., 2017).

506 It is yet to be fully understood whether local gut microbiota alterations directly contribute
507 to adverse outcomes in aged frail populations. Complementing *in vitro* findings, an *in vivo*
508 FMT approach reinforces the hypothesis that prefrailty associated microbes could directly
509 cause a sub-inflammatory phenotype in the gut. Although this aligns with other studies of
510 aged microbiota transfer (Parker et al., 2022), the novel message from the present study lies
511 in the separation between robustness and prefrailty-associated sampling. Here, we found
512 that macroscopic colon damage induced by aged microbiota may be more pronounced with
513 prefrail microbiota than with robust (Fig.6C). Undoubtedly, the interaction between the gut
514 microbiome and its host is bidirectional and more complex links are expected *in vivo*. A road
515 to be explored is the impact of a prefrailty microbiota within an aging host, where heightened
516 inflammatory stress and immunosenescence may compromise the host's ability to mount an
517 effective response to local insults (the inflammaging hypothesis (Franceschi et al., 2018)). In
518 addition to the virulent behavior of prefrail biofilm, local inflammation may significantly alter
519 microbial biotope making it less favorable to commensal gut bacteria, or even promoting the
520 blooming of pathogenic taxa (e.g., *Enterobacteriaceae* (Winter et al., 2013)). This could be
521 attributed to compromised epithelial secretory functions in high age, such as defective mucus
522 and antimicrobial peptide production(Sovran et al., 2019), or deficiencies in intestinal barrier
523 integrity (Man et al., 2015)– although the latter phenomenon remains a subject of debate
524 (Wilms et al., 2020). Natural polyphenols, including those present in grape pomace, have been

525 shown to improve cognitive function, extend the lifespan, and protect against age-related
526 muscle loss in several mice models (Davinelli & Scapagnini, 2022; Luo et al., 2021; Xu et al.,
527 2021; Ziegler et al., 2023). Studies in mice have shown that grape pomace in the diet can
528 improve metabolic diseases by preventing gut microbiota dysbiosis and increasing the
529 abundance of beneficial taxa (Chacar et al., 2018; Mezhibovsky et al., 2023; Roopchand et al.,
530 2015). In this study, we found that an industrial grape pomace preparation favored the
531 restoration of the physical and non-pathogenic features of biofilms *in vitro*, potentially
532 indicating the improved resilience of microb-aging communities (Fig.7). Additionally, this
533 compound reduced the release of proinflammatory triggering bacteria from prefrail biofilms.
534 Previous study suggested that grape pomace did not cause a significant taxonomic shift in
535 human gut microbiota (Ramos-Romero et al., 2020). Therefore, further research is needed to
536 determine the precise impact of grape polyphenols on microbial virulence functions and to
537 elucidate specific microbial genetic responses. Finally, going beyond this particular
538 compound, the methodology presented here may support the clinical relevance of gut
539 microbiota biofilm cultures (using non-invasive fecal samples) to assess and validate the
540 effects of new classes of geroprotectors, such as prebiotics or probiotics, specifically targeting
541 signs of unhealthy microb-aging.

542 **5. CONCLUSION**

543 Beyond the well-known taxonomic changes in the aging gut microbiome, this study points to
544 novel functional and behavioral changes in human gut biofilm, that switched to a virulent
545 phenotype in prefrail individuals but not in robusts. Importantly, we found that this
546 phenotype was reversible by prebiotic treatment. Altogether, these results further establish
547 the intestinal microbiota as a target to improve healthy aging. These discoveries might

548 represent a unique opportunity for geroclinicians to develop screening tools and identify new
549 therapeutic targets against microb-aging, to prevent frailty development in the expanding
550 aging population.

551 **Author Contributions:** GLC. performed most experiments, analyzed data, and provided
552 clinical input; MP., EM., JT., CD., NV. and JPM. contributed to *in vivo* and *in vitro* data
553 acquisition and analysis; SG., and BV. provided human samples, contributed to clinical
554 characterization, and reviewed manuscript; YS., BG., and A.P provided mice samples,
555 contributed to clinical characterization and reviewed manuscript; LB., BB. reviewed
556 manuscript and provided clinical input; JPM. performed 16S bioinformatics and statistics;
557 GLC., NV. and JPM., wrote the manuscript; N.V and JPM. supervised the work and obtained
558 fundings. All authors have read and agreed the final version of the manuscript.

559 **Funding:** Fundings came from INSPIRE-Grant AMIGO / ANR dysBIOFILM ANR-22-CE14-
560 0041-01 (JPM), ANR-PARCURE PRCE-CE18, 2020 (NV), and the national program "Microbiote"
561 from INSERM (NV and JPM). The INSPIRE-T study was supported by grants from the Region
562 Occitanie/Pyrénées-Méditerranée (Reference number: 1901175), the European Regional
563 Development Fund (ERDF) (Project number: MP0022856), and the Inspire Chairs of Excellence
564 funded by: Alzheimer Prevention in Occitania and Catalonia (APOC), EDENIS, KORIAN, Pfizer,
565 Pierre-Fabre.

566 **Data Availability Statement:** 16S rDNA sequences from the experimental biofilms and
567 mouse data were uploaded to the NCBI Sequence Read Archive (SRA Bioproject
568 PRJNA1076354). Additional biological or clinical metadata from the INSPIRE-T cohort can be
569 obtained by contacting the corresponding author, who will submit the request to the INSPIRE
570 biobanking and research committee for final approval. Other information from this study can
571 be obtained, upon reasonable requests, from the corresponding author.

572 **Ethics:** The INSPIRE cohort protocol ID NCT04224038 was approved by the French Ethical
573 Committee located in Rennes (CPP Ouest V) in October 2019. Mice experimentation protocol

574 has been approved by local ethic committee of Toulouse University and by the Ministry of
575 Superior Education and Research under the agreement APAFIS2023060610225611.

576 **Acknowledgments:** Authors thank the Department of Gastroenterology and
577 Pancreatology at the University Hospital of Toulouse for an MD/PhD scholarship leave to GLC.
578 Authors give credit to Dr. Felipe Sierra for its initial assessment of the research project, under
579 the umbrella of INSPIRE Call for Geroscience Research Grant. Authors thank the INSPIRE
580 biobanking committee for evaluating our project and approving sample collection. Authors
581 thank the staff of the human and mice Centre de Recherche Biologique (CRB) of the Toulouse
582 Hospital for samples preparation. Authors thank the CREFFRE core facility (UMS 006) for
583 hosting animals used in the project and contributing to histopathology analyses (R. Balouzat
584 and S. Milia), and the TRI-Genotoul platform for cellular imaging facilities (U1043, S. Allart).
585 Authors are thankful to Dr. Racaud-Sultan for critically reading the manuscript.

586 **Conflicts of Interest:** Prebiotic product (grape pomace) was gratuitously furnished by the
587 NEXIRA company (Rouen, France) and covered by a collaborative research grant between DG.
588 and NV. The company acknowledges having no influence on the results obtained during
589 assays presented in this manuscript.

	Adults (30-70 yrs) (n=13)	>70yrs robusts (n=15)	>70yrs prefrails (n=14)	p
Gender				0.846
Male	7 (53.8)	6 (42.9)	7 (46.7)	
Female	6 (46.2)	8 (57.1)	8 (53.3)	
Mean age (years)	47.8 (±11.6)	77.8 (±5.21)[1]	76.2 (±5.07)	**< 0.001**
Household status				0.786
Solo	9 (69.2)	10 (71.4)	9 (60)	
With partner	4 (30.8)	4 (28.6)	6 (40)	
Mean Fried Frailty Index	0 (±0)	0 (±0)[2]	1.14 (±0.363)	**< 0.001**
Mean Charlson Comorbidity Index	0.923 (±1.19)	5.07 (±1.59)[3]	4.73 (±1.87)	**< 0.001**
Mean MNA score	27.7 (±1.58)	28.1 (±1.27)	27.5 (±2.30)	0.713

590 **Table 1. Human cohort characteristics.** Data are represented as mean (± standard deviation) for continuous variables and n (%) for categorical
591 variables. MNA: Mini nutritional assessment. Statistical significance was determined by ANOVA (Fisher test) followed by Tukey's for multiple
592 comparisons for continuous variables and Chi squared test for categorical varibales, where P<0.05 was considered significant. [1] Prefrail vs robust
593 (p= 0.846) and Prefrail vs Adults (p< 0.001), [2] Prefrail vs robust (p< 0.001) and Prefrail vs Adults (p< 0.001), [3] Prefrail vs robust (p= 0.836) and
594 Prefrail vs Adults (p< 0.001)
595

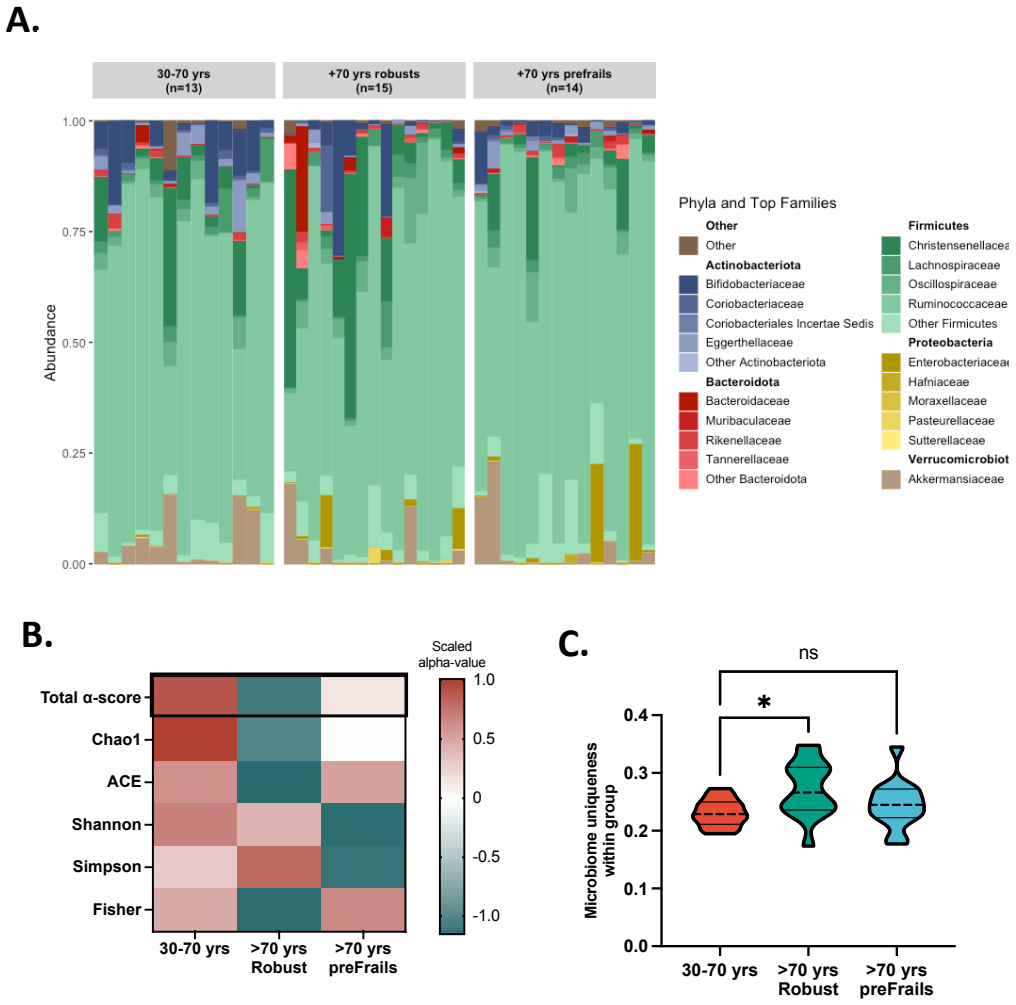
A.
30-70 yrs (n=13)
+70 yrs robusts (n=15)
+70 yrs prefrails (n=14)
Abundance
1.00
0.75
0.50
0.25
0.00
Phyla and Top Families
Other
Other
Actinobacteriota
Bifidobacteriaceae
Coriobacteriaceae
Coriobacteriales Incertae Sedis
Eggerthellaceae
Other Actinobacteriota
Bacteroidota
Bacteroidaceae
Muribaculaceae
Rikenellaceae
Tannerellaceae
Other Bacteroidota
Firmicutes
Christensenellaceae
Lachnospiraceae
Oscillospiraceae
Ruminococcaceae
Other Firmicutes
Proteobacteria
Enterobacteriaceae
Hafniaceae
Moraxellaceae
Pasteurellaceae
Sutterellaceae
Verrucomicrobiot
Akkermansiaceae
B.
Scaled alpha-value
1.0
0.5
0
-0.5
-1.0
Total α-score
Chao1
ACE
Shannon
Simpson
Fisher
30-70 yrs
>70 yrs Robust
>70 yrs preFrails
C.
ns
*
Microbiome uniqueness within group
0.4
0.3
0.2
0.1
0.0
30-70 yrs
>70 yrs Robust
>70 yrs preFrails
D.
f_Tannerellaceae
g_Parabacteroides
g_Parasutterella
o_Burkholderiales
f_Sutterellaceae
o_Bacteroidales
p_Bacteroidota
c_Bacteroidia
g_Monoglobus
o_Monoglobales
f_Monoglobaceae
g_Bilophila
g_Eubacterium_ventriosum_group
g_Oscillibacter
o_Bifidobacteriales
p_Actinobacteriota
g_Butyricimonas
f_Eggerthellaceae
c_Coriobacteriia
o_Coriobacteriales
g_Enterorhabdus
g_Dialister
g_Lactococcus
o_Eubacteriales
f_Veillonellaceae
g_Senegalimassilia
g_Negativibacillus
g_Slackia
f_Butyricicoccaceae
g_Butyricicoccus
f_Eubacterium_coprostanoligenes_g
o_Lachnospirales
f_Lachnospiraceae
f_Pasteurellaceae
g_Haemophilus
Household
Gender
MNA score
Fried score
Charlson index
Age
Correlation
positive
neutral
negative

597 **Fig.1: Taxonomic analyses of biofilms from human aging cohort.** Fecal microbiota cultured *in vitro* on a polymicrobial anaerobic biofilm
598 model underwent 16S rDNA metabarcoding targeting V3-V4 regions. The study groups include individuals aged 30-70 years (n=13),
599 individuals aged 70 years and above characterized as healthy aging (robust, n=15) and +70 years prefrail (n=14). **A.** The stacked bar plots
600 illustrate the relative abundance of the 5 major Phyla and their top 5 most abundant Families. Each individual is depicted as a separate bar
601 plot, highlighting taxonomic variations. **B.** The heatmap displays scaled mean values of five alpha-diversity indices calculated for each
602 individual within the three study groups. The first row, representing combined total alpha diversity. **C.** For each individual, the average of
603 lowest values from four different beta-diversity matrices (Bray-Curtis, Jaccard, unifrac, and weighted unifrac) represented individual
604 uniqueness. Statistical significance was determined by ANOVA followed by Tukey's for multiple comparisons, where P<0.05 was considered
605 significant (* for P< 0.05, *** for P<0.0010). **D.** Heatmap represents Kendall's correlation coefficients between biofilm taxa counts clinical
606 parameters from human donors. Clinical parameters include discrete and continuous clinical features: household (1: solo 2: with a partner),
607 gender (1: male, 2: female), MNA score, Charlson index, age, and Fried Frailty Index. The color gradient from blue to red signifies negative to
608 positive correlations, and * corresponds to Kendall's P value <0.05. For enhanced clarity, the heatmap was filtered to include only significantly
609 positive or negative correlations (P<0.05).

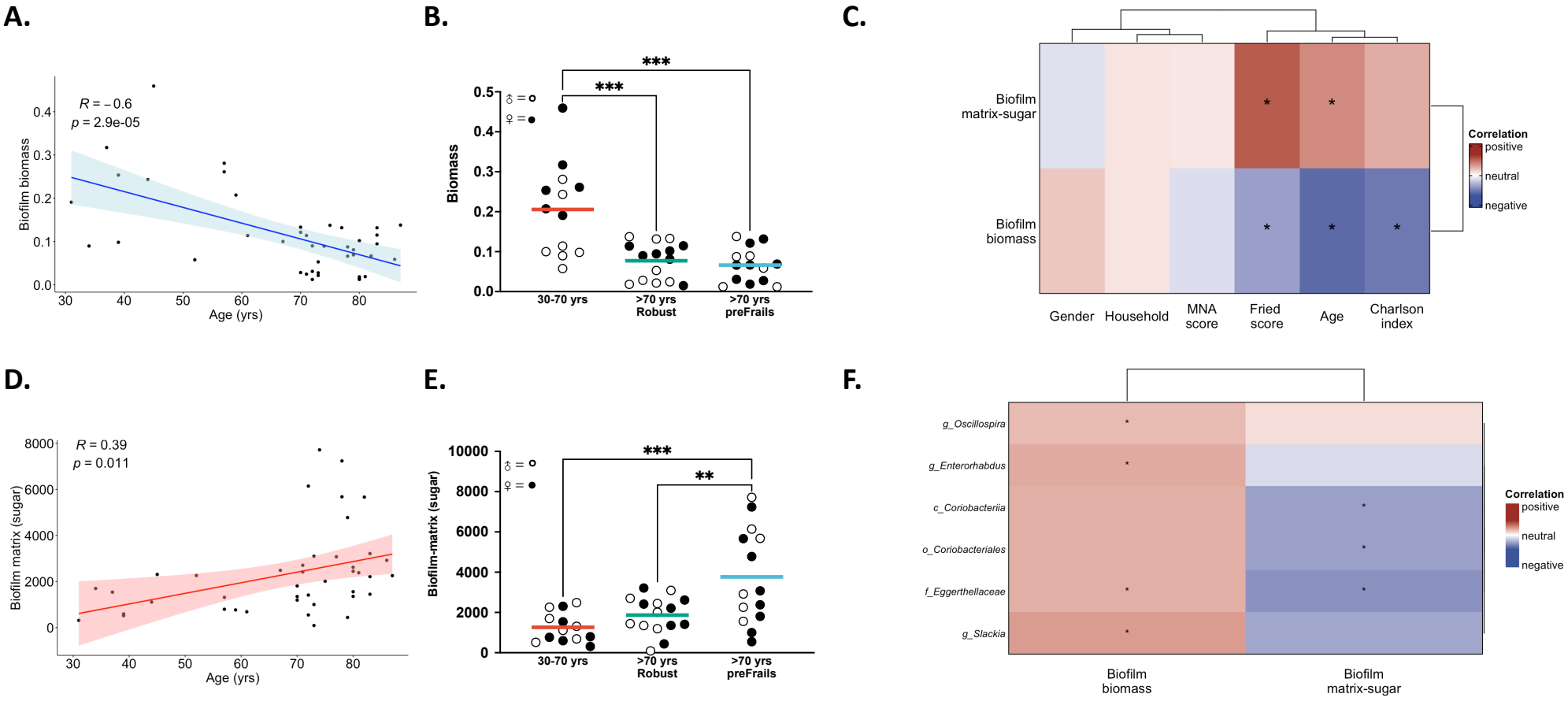
A.
R = −0.6
p = 2.9e-05
Biofilm biomass
Age (yrs)
B.
***
***
♂ = ○
♀ = ●
Biomass
30-70 yrs
>70 yrs Robust
>70 yrs preFrails
C.
Biofilm matrix-sugar
Biofilm biomass
Gender
Household
MNA score
Fried score
Age
Charlson index
Correlation
positive
neutral
negative
D.
R = 0.39
p = 0.011
Biofilm matrix (sugar)
Age (yrs)
E.
***
**
♂ = ○
♀ = ●
Biofilm-matrix (sugar)
30-70 yrs
>70 yrs Robust
>70 yrs preFrails
F.
g_Oscillospira
g_Enterorhabdus
c_Coriobacteriia
o_Coriobacteriales
f_Eggerthellaceae
g_Slackia
Biofilm biomass
Biofilm matrix-sugar
Correlation
positive
neutral
negative

611 **Fig.2. Prefrailty associated microb-aging is linked with physical alterations of human biofilms.** Feces from individuals aged 30-70 years,
612 70+ years robust, and 70+ years prefrail, were cultured *in vitro* as a polymicrobial anaerobic biofilm. **(A-B)** The total biofilm biomass and **(D-**
613 **E)** and the total sugar content of extracellular biofilm matrix were measured. **(A-D)** Pearson correlation relationship between biofilm
614 measures (biomass in **A.**, sugar-matrix in **D.**) and donor's age are presented. Shaded area around the regression line represents the 95%
615 confidence interval. **(B-E)** Scatter plots depict for each individual's its corresponding value of biofilm biomass (in **B.**) and biofilm sugar-matrix
616 (in **E.**) and were grouped for each three cohort of individuals. In panels B and E each dot is the average value of an individual donor biofilm
617 (at least 12 replicates). The gender of each donor is indicated using open(male)/filled(female) circles. Statistical significance was determined
618 by ANOVA followed by Tukey's for multiple comparisons, where $P<0.05$ was considered significant. **(C-F)** Heatmaps represent Kendall (in **F.**)
619 or Pearson (in **C.**) correlation coefficients between biofilm physical structure and clinical data (in **C.**) or biofilm taxa counts (in **F.**). Clinical
620 parameters include discrete and continuous clinical features: household (1: solo 2: with a partner), gender (1: male, 2: female), MNA score,
621 Charlson index, age, and Fried Frailty Index. The color gradient from blue to red signifies negative to positive correlations, and * corresponds
622 to P value <0.05. For enhanced clarity, the heatmap in panel **F.** was filtered to include only significantly positive or negative correlations
623 ($P<0.05$).
624

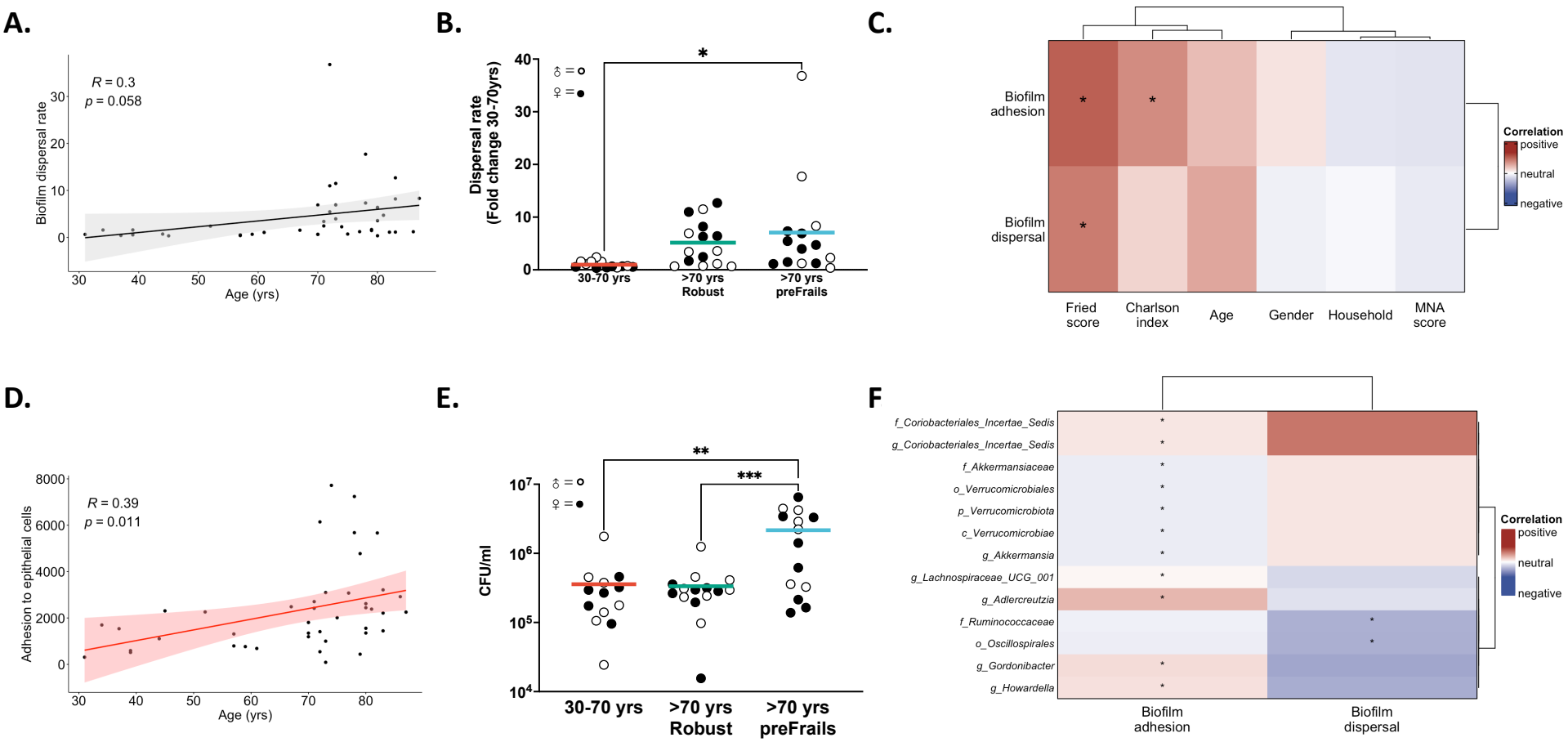
A.
R = 0.3
p = 0.058
Biofilm dispersal rate
Age (yrs)
B.
♂ = ○
♀ = ●
Dispersal rate (Fold change 30-70yrs)
30-70 yrs
>70 yrs Robust
>70 yrs preFrails
C.
Biofilm adhesion
Biofilm dispersal
Fried score
Charlson index
Age
Gender
Household
MNA score
Correlation
positive
neutral
negative
D.
R = 0.39
p = 0.011
Adhesion to epithelial cells
Age (yrs)
E.
CFU/ml
30-70 yrs
>70 yrs Robust
>70 yrs preFrails
F
f_Coriobacteriales_Incertae_Sedis
g_Coriobacteriales_Incertae_Sedis
f_Akkermansiaceae
o_Verrucomicrobiales
p_Verrucomicrobiota
c_Verrucomicrobiae
g_Akkermansia
g_Lachnospiraceae_UCG_001
g_Adlercreutzia
f_Ruminococcaceae
o_Oscillospirales
g_Gordonibacter
g_Howardella
Biofilm adhesion
Biofilm dispersal
Correlation
positive
neutral
negative

626 **Fig.3. Prefrailty associated microb-aging is linked with pathogenic traits of human biofilms.** Feces from individuals aged 30-70 years, 70+
627 years robust, and 70+ years prefrail, were cultured *in vitro* as a polymicrobial anaerobic biofilm. **(A-B)** The rate of dispersal of planktonic
628 bacteria, biofilm-dispersed bacteria, during a 24-hour period from biofilms was measured. Raw values were normalized to the average
629 dispersal rate of the 30-70 years group. **(D-E)** Normalized counts of biofilm-dispersed bacteria were cultured on the apical surface of the
630 human Caco2/HT29MTX monolayer. After a 4-hour coculture, the number of bacteria adhered to the epithelium was quantified. **(A-D)**
631 Pearson correlations between biofilm rate of dispersal (in **A.**) or adhesiveness (in **D.**) with the age of donors is presented. **(B-E)** Scatter plots
632 depict for each individual's its corresponding value of biofilm dispersal rate (in **B.**) or adhesiveness (in **E.**) and were grouped for each three
633 cohort of individuals. In panels B and E each dot is the average value of an individual donor biofilm (at least 12 replicates). The gender of
634 each donor is indicated using open(male)/filled(female) circles. Statistical significance was determined by ANOVA followed by Tukey's for
635 multiple comparisons, where $P<0.05$ was considered significant. **(C-F)** Heatmaps represent Kendall (in **F.**) or Pearson (in **C.**) correlation
636 coefficients between biofilm pathogenic traits and clinical data (in **C.**) or biofilm taxa counts (in **F.**). Clinical parameters include discrete and
637 continuous clinical features: household (1: solo 2: with a partner), gender (1: male, 2: female), MNA score, Charlson index, age, and Fried
638 Frailty Index. The color gradient from blue to red signifies negative to positive correlations, and * corresponds P value <0.05. For enhanced
639 clarity, the heatmap in panel **F.** was filtered to include only significantly positive or negative correlations ($P<0.05$).

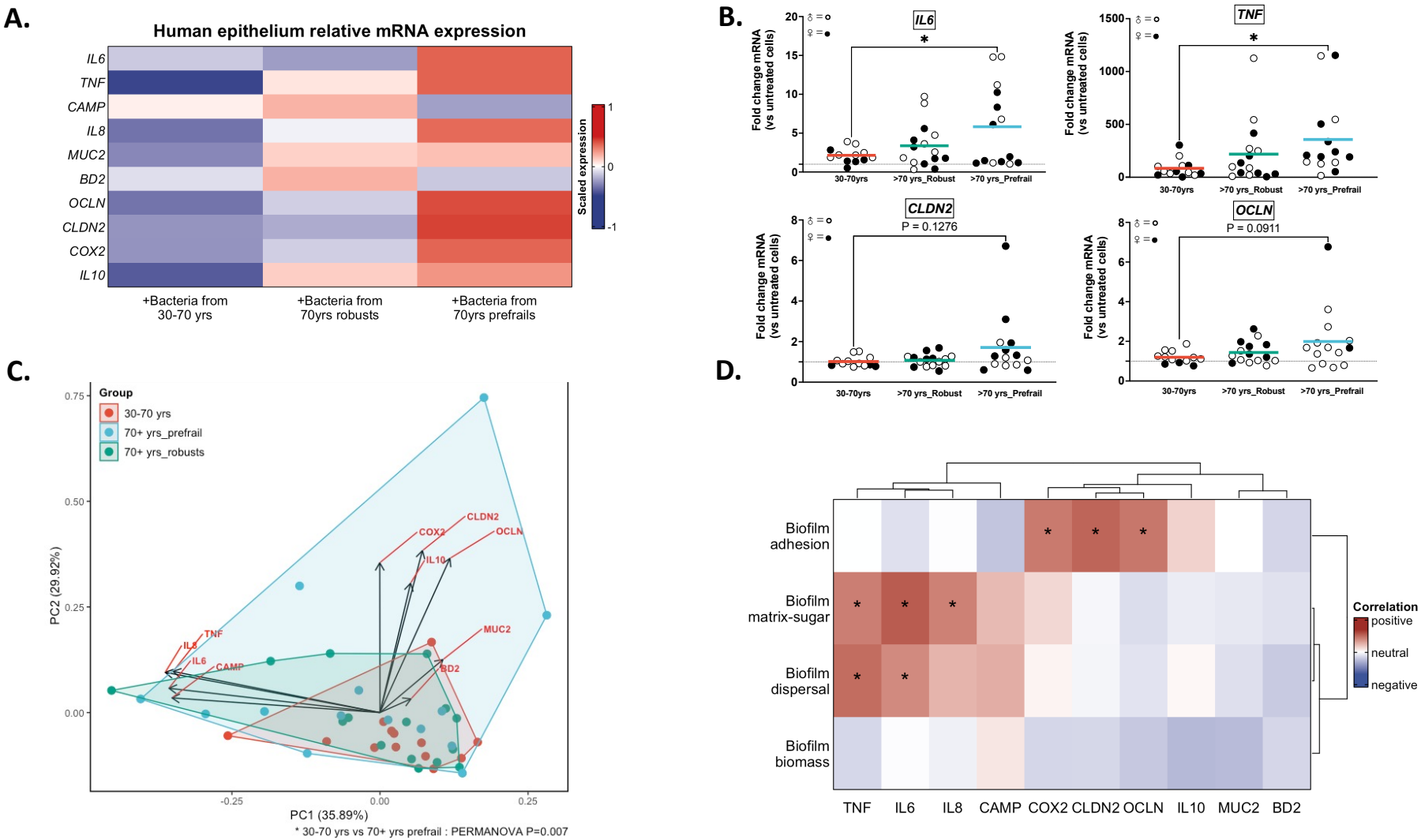
A.
Human epithelium relative mRNA expression
IL6
TNF
CAMP
IL8
MUC2
BD2
OCLN
CLDN2
COX2
IL10
+Bacteria from 30-70 yrs
+Bacteria from 70yrs robusts
+Bacteria from 70yrs prefrails
Scaled expression
B.
IL6
TNF
CLDN2
P = 0.1276
OCLN
P = 0.0911
Fold change mRNA (vs untreated cells)
30-70yrs
>70 yrs_Robust
>70 yrs_Prefrail
C.
Group
30-70 yrs
70+ yrs_prefrail
70+ yrs_robusts
PC2 (29.92%)
PC1 (35.89%)
* 30-70 yrs vs 70+ yrs prefrail : PERMANOVA P=0.007
D.
Biofilm adhesion
Biofilm matrix-sugar
Biofilm dispersal
Biofilm biomass
Correlation
positive
neutral
negative

641 **Fig.4. Increased host epithelial inflammatory response to prefrailty-associated human biofilms.** After coculture with a normalized
642 amount of biofilm-dispersed bacteria, epithelial cells were collected for RNA extraction. **A.** The heatmap represents scaled relative expression
643 of a targeted list of host response genes. Specifically, these genes are involved in innate inflammatory signaling (*IL6*, *TNF*, *IL8*, *IL10*, *COX2*,
644 and *BD2*), secretion (*BD2* and *MUC2*), and tight junction function (*OCLN* and *CLDN2*). The color gradient from blue to red correspond to scale
645 relative mRNA expression. **B.** Scatter plot depicts relative mRNA expression of *IL6*, *TNF*, *CLDN2* and *OCLN* for each individual's and were
646 grouped for each three cohort of individuals. The gender of each donor is indicated using open(male)/filled(female) circles. Dotted line at 1
647 corresponds to basal mRNA expression in wells without bacteria. Statistical significance was determined by ANOVA followed by Tukey's for
648 multiple comparisons, where $P<0.05$ was considered significant. **C.** Gene expression dataset was ordinated using Principal Component
649 Analysis (PCA) with its corresponding bi-plot vectors. Pairwise PERMANOVA revealed statistical differences between the group of 30-70 years
650 and +70 years prefrail ($P=0.007$). **D.** The heatmap corresponds to Pearson correlation coefficients between host epithelial gene response and
651 biofilm features. The color gradient from blue to red signifies negative to positive correlations, and * corresponds to Pearson P value <0.05.

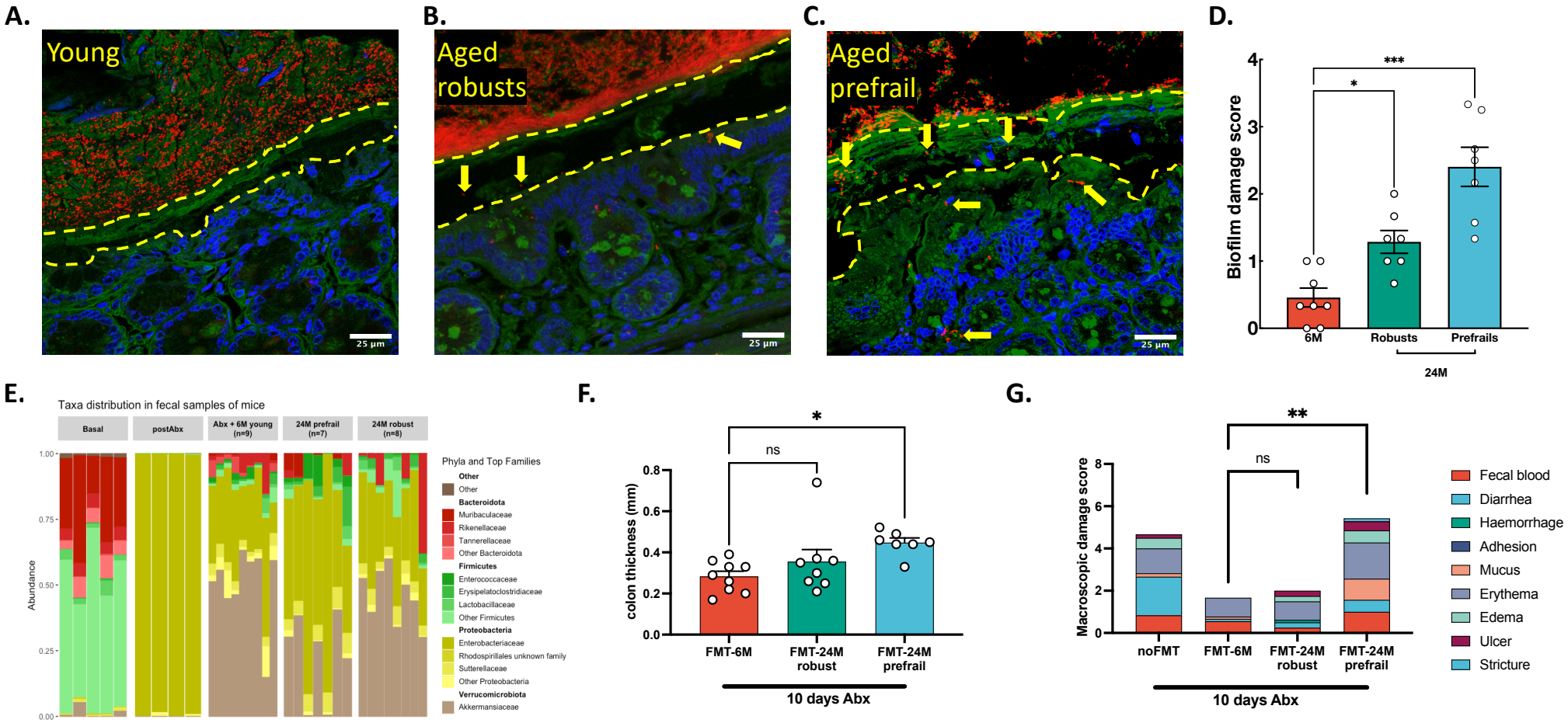
A.
Young
25 µm
B.
Aged robusts
25 µm
C.
Aged prefrail
25 µm
D.
Biofilm damage score
***
*
6M
Robusts
Prefrails
24M
E.
Taxa distribution in fecal samples of mice
Basal
postAbx
Abx + 6M young (n=9)
24M prefrail (n=7)
24M robust (n=8)
Abundance
Phyla and Top Families
Other
Bacteroidota
Muribaculaceae
Rikenellaceae
Tannerellaceae
Other Bacteroidota
Firmicutes
Enterococcaceae
Erysipelatoclostridiaceae
Lactobacillaceae
Other Firmicutes
Proteobacteria
Enterobacteriaceae
Rhodospirillales unknown family
Sutterellaceae
Other Proteobacteria
Verrucomicrobiota
Akkermansiaceae
F.
colon thickness (mm)
*
ns
FMT-6M
FMT-24M robust
FMT-24M prefrail
10 days Abx
G.
Macroscopic damage score
**
ns
noFMT
FMT-6M
FMT-24M robust
FMT-24M prefrail
10 days Abx
Fecal blood
Diarrhea
Haemorrhage
Adhesion
Mucus
Erythema
Edema
Ulcer
Stricture

653 **Fig.5. Prefrailty aging in mice is linked with altered gut biofilm and emergence of pathogenic behavior when transferred into recipient mice.**

654 **(A-C.)** Using 16S rDNA fluorescent *in situ* hybridization, we visualized tissue-associated microbiota in the distal colon of young (6 months, 6M,

655 n=8, A.), aged (24 months, 24M) robust (n=7, B.), and aged prefrail (n=7, **C.**) mice. Representative images are presented with blue is DAPI staining

656 for host nuclei, green is fluorescein-coupled wheat germ agglutinin for sugar-rich content (e.g., mucus layer), and red is the 16S-Cyanine3 probe

657 for all bacteria. Dashed lines represent the limits of mucosal tissue and the "inner mucus layer". Arrows highlight areas of interest. Scale bars

658 are 25 µm.**D.** Biofilm-damage scores were calculated for the three groups of mice, with dots representing the mean score from at least 3 fields

659 per animal. **(E-G.)** C57Bl/6 animals (8 weeks old) were previously exposed to 10-day antibiotics and underwent oral gavage with feces (fecal

660 microbiota transplantation, FMT) from young (FMT-6M, n=9), aged robust (FMT-24M robust, n=8), and aged prefrail (FMT-24M prefrail, n=7)

661 mice. **E.** Four days after transplantation, feces were collected for microbial taxonomy assessment using 16S rDNA metabarcoding. Colons were

662 harvested for (**F.**) parietal thickness measurement and (**G.**) macroscopic damage score. **(D, F, G)** Bar plots corresponds to mean value per group

663 ±SEM. Statistical significance was determined by ANOVA followed by Dunnett's for multiple comparisons, where $P<0.05$ was considered

664 significant (* for $P<0.05$, ** for $P<0.01$).

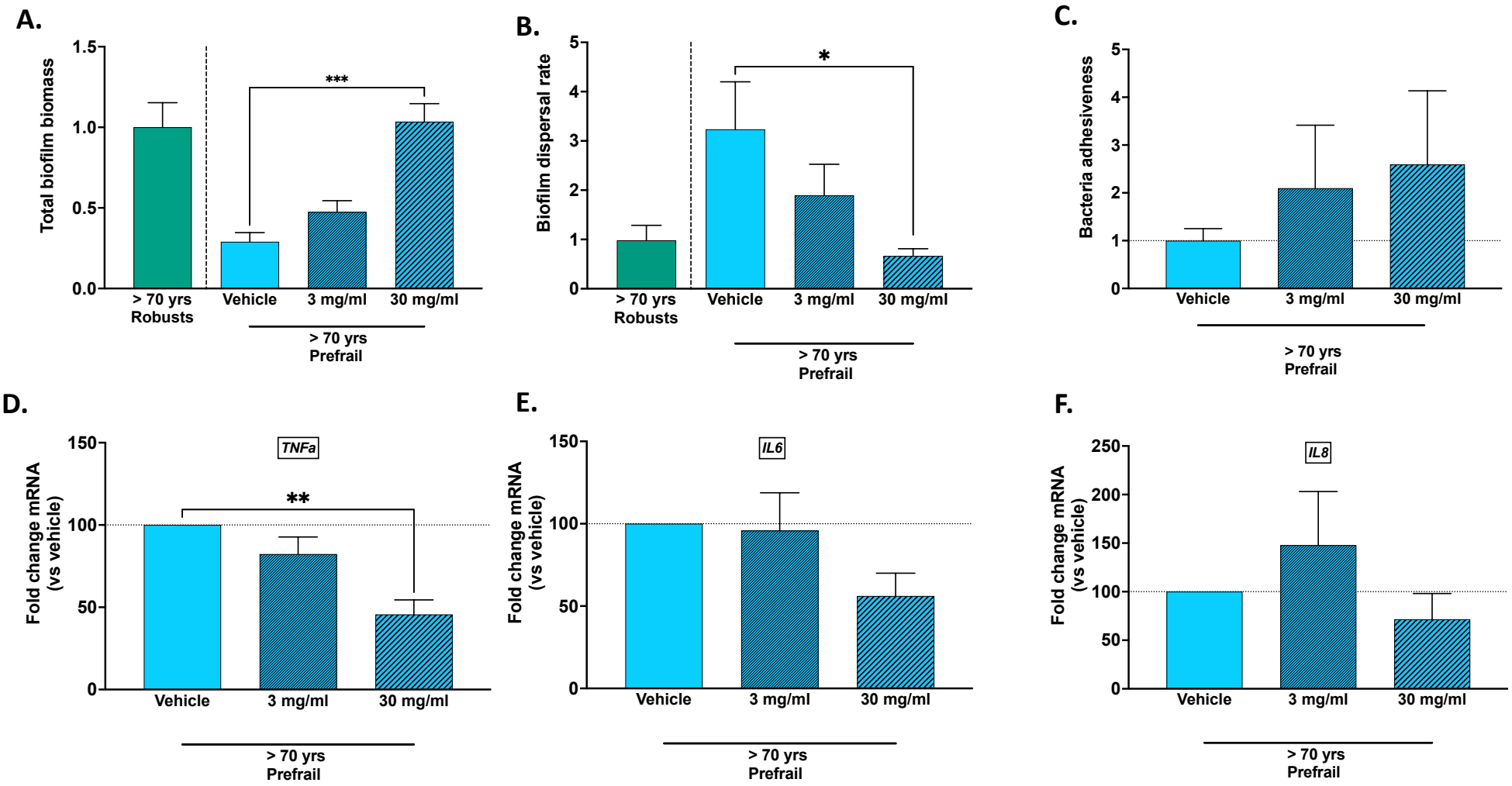
A.
Total biofilm biomass
1.5
1.0
0.5
0.0
***
> 70 yrs Robusts
Vehicle
3 mg/ml
30 mg/ml
> 70 yrs Prefrail
B.
Biofilm dispersal rate
5
4
3
2
1
0
*
> 70 yrs Robusts
Vehicle
3 mg/ml
30 mg/ml
> 70 yrs Prefrail
C.
Bacteria adhesiveness
5
4
3
2
1
0
Vehicle
3 mg/ml
30 mg/ml
> 70 yrs Prefrail
D.
TNFa
Fold change mRNA (vs vehicle)
150
100
50
0
**
Vehicle
3 mg/ml
30 mg/ml
> 70 yrs Prefrail
E.
IL6
Fold change mRNA (vs vehicle)
150
100
50
0
Vehicle
3 mg/ml
30 mg/ml
> 70 yrs Prefrail
F.
IL8
Fold change mRNA (vs vehicle)
250
200
150
100
50
0
Vehicle
3 mg/ml
30 mg/ml
> 70 yrs Prefrail

666

667 **Fig.6 Positive impact of grape pomace on prefrailty-associated human biofilm structure and virulence.** Polymicrobial anaerobic biofilms
668 were generated from human donor feces (30-70yrs old, >70yrs robust; >70yrs prefrail, n=4 per group) and exposed to grape pomace diluted
669 in microbial broth at concentrations of 3 to 30 mg/ml for 24 hours. **A.** Total biomass was evaluated using safranin-O stain, and the data are
670 presented as the fold change of mean biomass from individuals aged 30-70 years. **B.** The rate of dispersal for each biofilm was evaluated as a
671 ratio between amount of biofilm-dispersed bacteria and biofilm biomass previously assessed. **C.** Normalized counts of biofilm-dispersed
672 bacteria were cultured on the apical surface of the human Caco2/HT29MTX monolayer. After a 4-hour coculture, the number of bacteria
673 adhered to the epithelium was quantified. **D-F**. Dispersed bacteria were collected from biofilms previously exposed to grape pomace. Human
674 intestinal epithelial cell lines (Caco2 and HT29MTX, at a 3:1 ratio) were then exposed to these bacteria for 4 hours, and mRNA expression of
675 *TNF* (**D.**), *IL6* (**E.**) and *IL8* (**F.**) genes were assessed. **(A-C)** Bar plots corresponds to average value ± SEM of 12 biofilm replicates from human
676 donors (n=4). **(D-F)** Bar plots corresponds to average value ± SEM of relative mRNA expression of vehicle control group (n=4 human donors).
677 Statistical significance was determined by ANOVA followed by Dunnett's for multiple comparisons, where $P<0.05$ was considered significant
678 and * for $P<0.05$ and *** for $P<0.001$.

679 **References**

680 Ader, I., Penicaud, L., Andrieu, S., Beard, J. R., Davezac, N., Dray, C., . . . Casteilla, L. (2021).
681 Healthy Aging Biomarkers: The INSPIRE's Contribution. *The Journal of Frailty & Aging, 10*(4),
682 313-319. doi:10.14283/jfa.2021.15

683 Bernard, M., Rue, O., Mariadassou, M., & Pascal, G. (2021). FROGS: a powerful tool to analyse
684 the diversity of fungi with special management of internal transcribed spacers. *Brief*
685 *Bioinform, 22*(6). doi:10.1093/bib/bbab318

686 Biagi, E., Franceschi, C., Rampelli, S., Severgnini, M., Ostan, R., Turroni, S., . . . Candela, M.
687 (2016). Gut Microbiota and Extreme Longevity. *Current biology: CB, 26*(11), 1480-1485.
688 doi:10.1016/j.cub.2016.04.016

689 Biagi, E., Nylund, L., Candela, M., Ostan, R., Bucci, L., Pini, E., . . . De Vos, W. (2010). Through
690 ageing, and beyond: gut microbiota and inflammatory status in seniors and centenarians.
691 *PLoS ONE, 5*(5), e10667. doi:10.1371/journal.pone.0010667

692 Bosco, N., & Noti, M. (2021). The aging gut microbiome and its impact on host immunity.
693 *Genes Immun, 22*(5-6), 289-303. doi:10.1038/s41435-021-00126-8

694 Cani, P. D., Depommier, C., Derrien, M., Everard, A., & de Vos, W. M. (2022). Author
695 Correction: Akkermansia muciniphila: paradigm for next-generation beneficial
696 microorganisms. *Nat Rev Gastroenterol Hepatol, 19*(10), 682. doi:10.1038/s41575-022-
697 00650-6

698 Chacar, S., Itani, T., Hajal, J., Saliba, Y., Louka, N., Faivre, J. F., . . . Fares, N. (2018). The Impact
699 of Long-Term Intake of Phenolic Compounds-Rich Grape Pomace on Rat Gut Microbiota. *J*
700 *Food Sci, 83*(1), 246-251. doi:10.1111/1750-3841.14006

701 Charlson, M. E., Pompei, P., Ales, K. L., & MacKenzie, C. R. (1987). A new method of classifying
702 prognostic comorbidity in longitudinal studies: development and validation. *J Chronic Dis,*
703 *40*(5), 373-383. doi:10.1016/0021-9681(87)90171-8

704 Davinelli, S., & Scapagnini, G. (2022). Interactions between dietary polyphenols and aging gut
705 microbiota: A review. *Biofactors, 48*(2), 274-284. doi:10.1002/biof.1785

706 de Souto Barreto, P., Guyonnet, S., Ader, I., Andrieu, S., Casteilla, L., Davezac, N., . . . Vellas,
707 B. (2021). The INSPIRE Research Initiative: A Program for GeroScience and Healthy Aging
708 Research Going from Animal Models to Humans and the Healthcare System. *The Journal of*
709 *Frailty & Aging, 10*(2), 86-93. doi:10.14283/jfa.2020.18

710 DeJong, E. N., Surette, M. G., & Bowdish, D. M. E. (2020). The Gut Microbiota and Unhealthy
711 Aging: Disentangling Cause from Consequence. *Cell Host Microbe, 28*(2), 180-189.
712 doi:10.1016/j.chom.2020.07.013

713 Flemming, H. C., & Wingender, J. (2010). The biofilm matrix. *Nature Reviews Microbiology,*
714 *8*(9), 623-633. doi:10.1038/nrmicro2415

715 Franceschi, C., Garagnani, P., Parini, P., Giuliani, C., & Santoro, A. (2018). Inflammaging: a new
716 immune-metabolic viewpoint for age-related diseases. *Nature Reviews. Endocrinology,*
717 *14*(10), 576-590. doi:10.1038/s41574-018-0059-4

718 Fried, L. P., Tangen, C. M., Walston, J., Newman, A. B., Hirsch, C., Gottdiener, J., . . .
719 Cardiovascular Health Study Collaborative Research, G. (2001). Frailty in older adults:
720 evidence for a phenotype. *The Journals of Gerontology. Series A, Biological Sciences and*
721 *Medical Sciences, 56*(3), M146-156. doi:10.1093/gerona/56.3.m146

722 Ghosh, T. S., Shanahan, F., & O'Toole, P. W. (2022). The gut microbiome as a modulator of
723 healthy ageing. *Nat Rev Gastroenterol Hepatol, 19*(9), 565-584. doi:10.1038/s41575-022-
724 00605-x

725 Gill, T. M., Gahbauer, E. A., Allore, H. G., & Han, L. (2006). Transitions between frailty states
726 among community-living older persons. *Arch Intern Med, 166*(4), 418-423.
727 doi:10.1001/archinte.166.4.418

728 Gomez-Cabrera, M. C., Garcia-Valles, R., Rodriguez-Manas, L., Garcia-Garcia, F. J., Olaso-
729 Gonzalez, G., Salvador-Pascual, A., . . . Vina, J. (2017). A New Frailty Score for Experimental
730 Animals Based on the Clinical Phenotype: Inactivity as a Model of Frailty. *The Journals of*
731 *Gerontology. Series A, Biological Sciences and Medical Sciences, 72*(7), 885-891.
732 doi:10.1093/gerona/glw337

733 Jackson, M. A., Jeffery, I. B., Beaumont, M., Bell, J. T., Clark, A. G., Ley, R. E., . . . Steves, C. J.
734 (2016). Signatures of early frailty in the gut microbiota. *Genome Medicine, 8*(1), 8.
735 doi:10.1186/s13073-016-0262-7

736 Karygianni, L., Ren, Z., Koo, H., & Thurnheer, T. (2020). Biofilm Matrixome: Extracellular
737 Components in Structured Microbial Communities. *Trends Microbiol, 28*(8), 668-681.
738 doi:10.1016/j.tim.2020.03.016

739 Kong, F., Hua, Y., Zeng, B., Ning, R., Li, Y., & Zhao, J. (2016). Gut microbiota signatures of
740 longevity. *Current biology: CB, 26*(18), R832-R833. doi:10.1016/j.cub.2016.08.015

741 Langille, M. G., Meehan, C. J., Koenig, J. E., Dhanani, A. S., Rose, R. A., Howlett, S. E., & Beiko,
742 R. G. (2014). Microbial shifts in the aging mouse gut. *Microbiome, 2*(1), 50.
743 doi:10.1186/s40168-014-0050-9

744 Le Cosquer, G., Vergnolle, N., & Motta, J. P. (2024). Gut microb-aging and its relevance to
745 frailty aging. *Microbes Infect, 26*(3), 105309. doi:10.1016/j.micinf.2024.105309

746 Love, M. I., Huber, W., & Anders, S. (2014). Moderated estimation of fold change and
747 dispersion for RNA-seq data with DESeq2. *Genome Biol, 15*(12), 550. doi:10.1186/s13059-
748 014-0550-8

749 Luo, J., Si, H., Jia, Z., & Liu, D. (2021). Dietary Anti-Aging Polyphenols and Potential
750 Mechanisms. *Antioxidants (Basel), 10*(2). doi:10.3390/antiox10020283

751 Maffei, V. J., Kim, S., Blanchard, E. t., Luo, M., Jazwinski, S. M., Taylor, C. M., & Welsh, D. A.
752 (2017). Biological Aging and the Human Gut Microbiota. *The Journals of Gerontology. Series*
753 *A, Biological Sciences and Medical Sciences, 72*(11), 1474-1482. doi:10.1093/gerona/glx042

754 Man, A. L., Bertelli, E., Rentini, S., Regoli, M., Briars, G., Marini, M., . . . Nicoletti, C. (2015).
755 Age-associated modifications of intestinal permeability and innate immunity in human small
756 intestine. *Clin Sci (Lond), 129*(7), 515-527. doi:10.1042/CS20150046

757 Mandal, S., Van Treuren, W., White, R. A., Eggesbo, M., Knight, R., & Peddada, S. D. (2015).
758 Analysis of composition of microbiomes: a novel method for studying microbial composition.
759 *Microb Ecol Health Dis, 26*, 27663. doi:10.3402/mehd.v26.27663

760 Mezhibovsky, E., Tveter, K. M., Villa-Rodriguez, J. A., Bacalia, K., Kshatriya, D., Desai, N., . . .
761 Roopchand, D. E. (2023). Grape Polyphenols May Prevent High-Fat Diet-Induced Dampening
762 of the Hypothalamic-Pituitary-Adrenal Axis in Male Mice. *J Endocr Soc, 7*(9), bvad095.
763 doi:10.1210/jendso/bvad095

764 Motta, J. P., Allain, T., Green-Harrison, L. E., Groves, R. A., Feener, T., Ramay, H., . . . Buret, A.
765 G. (2018). Iron Sequestration in Microbiota Biofilms As A Novel Strategy for Treating
766 Inflammatory Bowel Disease. *Inflamm Bowel Dis, 24*(7), 1493-1502. doi:10.1093/ibd/izy116

767 Motta, J. P., Denadai-Souza, A., Sagnat, D., Guiraud, L., Edir, A., Bonnart, C., . . . Vergnolle, N.
768 (2019). Active thrombin produced by the intestinal epithelium controls mucosal biofilms. *Nat*
769 *Commun, 10*(1), 3224. doi:10.1038/s41467-019-11140-w

770 Motta, J. P., Flannigan, K. L., Agbor, T. A., Beatty, J. K., Blackler, R. W., Workentine, M. L., . . .
771 Wallace, J. L. (2015). Hydrogen sulfide protects from colitis and restores intestinal microbiota
772 biofilm and mucus production. *Inflamm Bowel Dis, 21*(5), 1006-1017.
773 doi:10.1097/MIB.0000000000000345

774 Motta, J. P., Wallace, J. L., Buret, A. G., Deraison, C., & Vergnolle, N. (2021). Gastrointestinal
775 biofilms in health and disease. *Nat Rev Gastroenterol Hepatol, 18*(5), 314-334.
776 doi:10.1038/s41575-020-00397-y

O'Toole, P. W., & Jeffery, I. B. (2015). Gut microbiota and aging. *Science (New York, N.Y.), 350*(6265), 1214-1215. doi:10.1126/science.aac8469

Parker, A., Romano, S., Ansorge, R., Aboelnour, A., Le Gall, G., Savva, G. M., . . . Carding, S. R. (2022). Fecal microbiota transfer between young and aged mice reverses hallmarks of the aging gut, eye, and brain. *Microbiome, 10*(1), 68. doi:10.1186/s40168-022-01243-w

Paulson, J. N., Stine, O. C., Bravo, H. C., & Pop, M. (2013). Differential abundance analysis for microbial marker-gene surveys. *Nat Methods, 10*(12), 1200-1202. doi:10.1038/nmeth.2658

Ramos-Romero, S., Martinez-Maqueda, D., Hereu, M., Amezqueta, S., Torres, J. L., & Perez-Jimenez, J. (2020). Modifications of Gut Microbiota after Grape Pomace Supplementation in Subjects at Cardiometabolic Risk: A Randomized Cross-Over Controlled Clinical Trial. *Foods, 9*(9). doi:10.3390/foods9091279

Robinson, M. D., McCarthy, D. J., & Smyth, G. K. (2010). edgeR: a Bioconductor package for differential expression analysis of digital gene expression data. *Bioinformatics, 26*(1), 139-140. doi:10.1093/bioinformatics/btp616

Rodriguez-Lopez, P., Rueda-Robles, A., Borrás-Linares, I., Quirantes-Piné, R. M., Emanuelli, T., Segura-Carretero, A., & Lozano-Sánchez, J. (2022). Grape and Grape-Based Product Polyphenols: A Systematic Review of Health Properties, Bioavailability, and Gut Microbiota Interactions. *Horticulturae, 8*(7), 583.

Rolland-Fourcade, C., Denadai-Souza, A., Cirillo, C., Lopez, C., Jaramillo, J. O., Desormeaux, C., . . . Vergnolle, N. (2017). Epithelial expression and function of trypsin-3 in irritable bowel syndrome. *Gut, 66*(10), 1767-1778. doi:10.1136/gutjnl-2016-312094

Romero-Ortuno, R., & Kenny, R. A. (2012). The frailty index in Europeans: association with age and mortality. *Age Ageing, 41*(5), 684-689. doi:10.1093/ageing/afs051

Roopchand, D. E., Carmody, R. N., Kuhn, P., Moskal, K., Rojas-Silva, P., Turnbaugh, P. J., & Raskin, I. (2015). Dietary Polyphenols Promote Growth of the Gut Bacterium Akkermansia

802 muciniphila and Attenuate High-Fat Diet-Induced Metabolic Syndrome. *Diabetes, 64*(8), 2847-
803 2858. doi:10.2337/db14-1916

804 Rubenstein, L. Z., Harker, J. O., Salva, A., Guigoz, Y., & Vellas, B. (2001). Screening for
805 undernutrition in geriatric practice: developing the short-form mini-nutritional assessment
806 (MNA-SF). *The Journals of Gerontology. Series A, Biological Sciences and Medical Sciences,*
807 *56*(6), M366-372. doi:10.1093/gerona/56.6.m366

808 Santin, Y., Lopez, S., Ader, I., Andrieu, S., Blanchard, N., Carriere, A., . . . Parini, A. (2021).
809 Towards a Large-Scale Assessment of the Relationship between Biological and Chronological
810 Aging: The INSPIRE Mouse Cohort. *The Journal of Frailty & Aging, 10*(2), 121-131.
811 doi:10.14283/jfa.2020.43

812 Segata, N., Izard, J., Waldron, L., Gevers, D., Miropolsky, L., Garrett, W. S., & Huttenhower, C.
813 (2011). Metagenomic biomarker discovery and explanation. *Genome Biol, 12*(6), R60.
814 doi:10.1186/gb-2011-12-6-r60

815 Sierra, F. (2016). The Emergence of Geroscience as an Interdisciplinary Approach to the
816 Enhancement of Health Span and Life Span. *Cold Spring Harb Perspect Med, 6*(4), a025163.
817 doi:10.1101/cshperspect.a025163

818 Sovran, B., Hugenholtz, F., Elderman, M., Van Beek, A. A., Graversen, K., Huijskes, M., . . .
819 Wells, J. M. (2019). Age-associated Impairment of the Mucus Barrier Function is Associated
820 with Profound Changes in Microbiota and Immunity. *Sci Rep, 9*(1), 1437. doi:10.1038/s41598-
821 018-35228-3

822 Wallace, J. L., Le, T., Carter, L., Appleyard, C. B., & Beck, P. L. (1995). Hapten-induced chronic
823 colitis in the rat: alternatives to trinitrobenzene sulfonic acid. *J Pharmacol Toxicol Methods,*
824 *33*(4), 237-239. doi:10.1016/1056-8719(95)00001-x

825 Wilmanski, T., Diener, C., Rappaport, N., Patwardhan, S., Wiedrick, J., Lapidus, J., . . . Price, N.
826 D. (2021). Gut microbiome pattern reflects healthy ageing and predicts survival in humans.
827 *Nature Metabolism, 3*(2), 274-286. doi:10.1038/s42255-021-00348-0

828 Wilms, E., Troost, F. J., Elizalde, M., Winkens, B., de Vos, P., Mujagic, Z., . . . Masclee, A. A. M.
829 (2020). Intestinal barrier function is maintained with aging - a comprehensive study in healthy
830 subjects and irritable bowel syndrome patients. *Sci Rep, 10*(1), 475. doi:10.1038/s41598-019-
831 57106-2

832 Winter, S. E., Winter, M. G., Xavier, M. N., Thiennimitr, P., Poon, V., Keestra, A. M., . . .
833 Baumler, A. J. (2013). Host-derived nitrate boosts growth of E. coli in the inflamed gut. *Science*
834 *(New York, N.Y.), 339*(6120), 708-711. doi:10.1126/science.1232467

835 World Health, O. (2020). *Decade of healthy ageing: baseline report*: World Health
836 Organization.

837 Xu, Q., Fu, Q., Li, Z., Liu, H., Wang, Y., Lin, X., . . . Sun, Y. (2021). The flavonoid procyanidin C1
838 has senotherapeutic activity and increases lifespan in mice. *Nature Metabolism, 3*(12), 1706-
839 1726. doi:10.1038/s42255-021-00491-8

840 Ziegler, T., Tsiountsioura, M., Meixner-Goetz, L., Cvirn, G., & Lamprecht, M. (2023).
841 Polyphenols' Impact on Selected Biomarkers of Brain Aging in Healthy Middle-Aged and
842 Elderly Subjects: A Review of Clinical Trials. *Nutrients, 15*(17). doi:10.3390/nu15173770

843